UTE STEMMER

Toxicity, uptake and targeting of oxidized phospholipids in cultured macrophages

DISSERTATION

zur Erlangung des akademischen Grades einer
Doktorin der technischen Wissenschaften

erreicht an der

Technischen Universität Graz

Betreuer:
Univ.-Prof. Dr. Albin Hermetter
Institut für Biochemie
Technische Universität Graz

2011

VORWORT

Die vorliegende Arbeit wurde in der Zeit von Mai 2007 bis Juli 2011 am Institut für Biochemie der Technischen Universität Graz durchgeführt.

Betreuer der Dissertation war Herr Prof. Dr. Albin Hermetter, dem ich an dieser Stelle danken möchte. Neben seinem herausragenden fachlichen Wissen und seinen Beiträgen, seiner tatkräftige Unterstützung und Hilfestellungen in allen Belangen, möchte ich mich für die vielen anregenden Diskussionen und vor allem auch für seine menschlichen Kompetenzen bedanken.

Ebenso gilt mein Dank der gesamten Arbeitsgruppe Hermetter für die gute Zusammenarbeit, den Zusammenhalt und die wertvollen Hilfestellungen.

Überdies möchte ich mich bei meiner ganzen Familie, allen voran meiner Mutter Christa, für den gegebenen Rückhalt über die gesamte Studiendauer hinweg bedanken. Mein Dank gilt auch meinem Freund Harald und seiner Familie für ihre großartige Unterstützung.

Ich widme diese Arbeit meinem Vater Siegfried, der im Gedanken stets bei mir ist.

STATUTORY DECLARATION

I declare that I have authored this thesis independently, that I have not used other than the declared sources / resources, and that I have explicitly marked all material which has been quoted either literally or by content from the used sources.

…… ……..
date (signature)

ABSTRACT

The uptake of oxidized low-density lipoprotein (oxLDL) by the macrophages of the arterial wall and the accumulation of apoptotic cells in atherosclerotic lesions are hallmarks of atherosclerosis. The harmful effects of oxLDL are largely mediated by the intrinsic toxicity of a great variety of lipid oxidation products that are generated in LDL under the conditions of oxidative stress. These compounds comprise oxidized sterols, oxidized fatty acid derivatives and oxidized glycerophospholipids. Oxidized phospholipids may contain a modified long-chain carboxylic acid or a truncated acyl residue with a polar functional group at its ω-end. Typical derivatives of truncated phospholipids are the carboxy-phospholipid 1-palmitoyl-2-glutaroyl-*sn*-glycero-3-phosphocholine (PGPC) and the chemically reactive aldehydo-phosphospholipid 1-palmitoyl-2-(5-oxovaleroyl)-*sn*-glycero-3-phosphocholine (POVPC), which are oxidation products of arachidonoyl-phosphatidylcholine. The latter lipid can undergo Schiff base formation with amino groups of proteins, thereby modulating their properties and functions.

It was the aim of the first part of this doctoral thesis to find out whether and to what extent the biological effects of oxLDL are mediated by truncated diacylphospholipids in cultured macrophages. For this purpose, we used chemically defined PGPC and POVPC as well as their natural 1-O-hexadecyl analogs and determined their toxicity in the macrophage-like cell line RAW 264.7 and bone marrow-derived macrophages (BMM). PGPC and POVPC induced apoptosis in both cell types, the bone marrow-derived cells being slightly more susceptible to phospholipid toxicity than the RAW 264.7 cells. POVPC rapidly activated an acid sphingomyelinase (aSMase) in cultured RAW 264.7 macrophages. If the expression of aSMase was abolished by a specific

inhibitor, the cells became more resistant to POVPC-induced apoptosis, showing that the activity of this enzyme is causally linked to POVPC toxicity in macrophages.

The second part of this doctoral thesis was devoted to the cellular uptake and the primary molecular targets of the oxidized phosphatidylcholines. For this purpose, we used the fluorescently-labeled analogs of PGPC and POVPC for visualization of lipids in live cells and lipid-protein complexes in acrylamide or agarose gels. The fluorescent analogs of PGPC and POVPC were easily taken up by the RAW 264.7 macrophages irrespective of the lipid presentation. Whereas POVPC was initially scavenged by covalent reaction with the components of the plasma membrane, PGPC was quickly internalized. Despite the covalent binding to its lipid and protein targets, POVPC is freely exchangeable between membranes and (lipo-) protein surfaces. As a consequence, this lipid represents a toxic compound which is active not only at the site of its formation but also in cells far distant from areas of oxidative stress. We isolated and identified the protein targets in cultured RAW 264.7 macrophages, which formed covalent Schiff base adducts with BY-POVPE. The respective polypeptides are involved in membrane transport, stress response, apoptosis and lipid metabolism. The identification of a considerable number of potential POVPC protein targets supports the assumption that POVPC interacts with multiple sites and not only with the traditional specific receptors.

KURZFASSUNG

Die Aufnahme von oxidierten Lipoproteinen geringer Dichte (oxLDL) durch Makrophagen in der Arterienwand und die Akkumulation von apoptotischen Zellen in atherosklerotischen Läsionen stellen Hauptkennzeichen der Atherosklerose dar. Die schädlichen Effekte von oxLDL werden zu einem großen Teil durch die spezifische Toxizität einer Reihe von Lipidoxidationsprodukten, die in LDL unter oxidativem Stress entstehen, vermittelt. Zu diesen Verbindungen gehören oxidierte Sterole, oxidierte Fettsäurederivate und oxidierte Glycerophospholipide. Oxidierte Phospholipide (oxPL) enthalten eine modifizierte langkettige Carbonsäure oder eine verkürzte Acylkette mit einer polaren Gruppe am ω- Ende. Zu den typischen Derivaten verkürzter Phospholipide aus der Oxidation von Arachidonoyl-Phosphocholin, gehören das Carboxy-Phospholipid 1-Palmitoyl-2-Glutaroyl-*sn*-glycero-3-phosphocholin (PGPC) und das chemisch-reaktive Aldehydo-Phospholipid 1-Palmitoyl-2-(5-Oxovaleroyl)-*sn-g*lycero-3-phosphocholin (POVPC). Das letztere Lipid kann mit Aminogruppen von Proteinen Schiff Basen bilden und damit deren Eigenschaften und Funktionen verändern.

Ziel des ersten Teiles dieser Doktorarbeit war es, die biologischen Effekte von oxLDL auf Makrophagen zu bestimmen, die durch verkürzte Diacylphospholipide vermittelt werden. Zu diesem Zweck wurde die Toxizität von chemisch definiertem PGPC und POVPC sowie der 1-O-hexadecyl- Analoga dieser Verbindungen in der Makrophagen Zelllinie RAW 264.7 und in Makrophagen aus Knochenmarkszellen (BMM), bestimmt. POVPC und PGPC lösten Apoptose in beiden Zelltypen aus, wobei die aus Knochenmarkszellen isolierten Makrophagen stärker beeinflusst wurden. Weiters aktivierte POVPC eine saure Sphingomyelinase (aSMase) in RAW 264.7 Makrophagen. Bei spezifischer Inhibition dieses Enzyms, konnte eine erhöhte

Resistenz der Zellen gegenüber POVPC-induzierter Apoptose festgestellt werden, was einen kausalen Zusammenhang zwischen Enzymaktivität und Zelltod aufzeigt.

Der zweite Teil dieser Doktorarbeit befasste sich mit der zellularen Aufnahme und den primären molekularen Targets von oxidierten Phosphatidylcholinen. Hierfür wurden die fluoreszenz-gelabelten Analoga von PGPC und POVPC verwendet, um die Lipide und Lipid-Protein Komplexe in lebenden Zellen und in Acrylamid- und Agarosegelen zu visualisieren. Die fluoreszierenden PGPC- und POVPC-Analoga wurden von den RAW 264.7 Zellen unabhängig von der Lipidpräsentation schnell aufgenommen. POVPC wurde über kovalente Reaktionen mit Plasmamembran-Komponenten in dieser zurückgehalten, wohingegen PGPC sehr schnell internalisiert wurde. Trotz der kovalenten Bindung an Proteine, ist POVPC zwischen Membran- und (Lipo-) Proteinoberflächen frei austauschbar. Daraus resultiert, dass dieses Lipid nicht nur an der Stelle seiner Bildung, sondern auch fern ab dem ursprünglichen oxidativen Stress wirken kann. Weiters wurden Proteintargets, die kovalente Addukte mit POVPC-Analoga bildeten, aus RAW 264.7 Makrophagen isoliert. Diese Proteine sind hauptsächlich in Transport, Stressantwort, Apoptose und Lipidmetabolismus involviert. Die Identifikation einer großen Anzahl der potentiellen Proteintargets unterstützt die Vermutung, dass POVPC, neben den traditionellen, spezifischen Rezeptoren, auch mit vielfältigen anderen Proteinmolekülen interagieren kann.

TABLE OF CONTENTS

CHAPTER 1

SUMMARY

1. Summary and Aims 12

2. References 19

CHAPTER 2

TOXICITY OF OXIDIZED PHOSPHOLIPIDS IN CULTURED MACROPHAGES

1. Abstract 22

2. Introduction 24

3. Materials and Methods 27

- **3.1** Materials 27
- **3.2** Cell culture 27
- **3.3** Assessment of BMM differentiation 28
- **3.4** Incubation of cells with oxPL 29
- **3.5** MTT viability assay 29
- **3.6** Flow cytometric apoptosis assay 30
- **3.7** Morphological studies 31
- **3.8** Proteins of apoptotic blebs 31
- **3.9** Time- dependent stability of oxPL 32
- **3.10** Acid sphingomyelinase activity 32
- **3.11** Statistical analysis 33

4. Results 34

5. Discussion 45

6. Abbreviations 50

7. Acknowledgements 52

8. References 53

CHAPTER 3

UPTAKE AND PROTEIN TARGETING OF FLUORESCENT OXIDIZED PHOSPHOLIPIDS IN CULTURED RAW 264.7 MACROPHAGES

1. Abstract 58

2. Introduction 60

3. Materials and Methods 63

3.1 Material 63

3.2 LDL isolation and modification 63

3.3 Delivery systems for fluorescently labeled oxPL 64

3.4 Cell culture 65

3.5 Fluorescence microscopy 65

3.5.1 Uptake of BY-oxPL in RAW 264.7 macrophages 65

3.5.2 Colocalization BY-oxPL with the plasma membrane 65

3.6 BY -POVPE exchange between cells, LDL and albumin 66

3.7 Determination of protein targets of BY -POVPE 66

3.7.1 Separation of total cell protein by 2-D electrophoresis 66

3.7.2 Separation of membrane proteins by 1-D gel electrophoresis 67

3.7.3 Tryptic digest and MS/MS analysis 69

4. Results 70

5. Discussion 84

6. Abbreviations 91

7. Acknowledgements 93

8. References 94

FIGURES AND TABLES:

CHAPTER 2

TOXICITY OF OXIDIZED PHOSPHOLIPIDS IN CULTURED MACROPHAGES

Figure 1: Chemical structures of oxidized phospholipids 34

Figure 2: Effects of oxPL on viability of RAW 264.7 and BMM 35

Figure 3: Morphological changes in RAW 264.7 macrophages 36

Figure 4: Apoptotic effects of oxPL in RAW 264.7 and BMM 38

Figure 5: Time- dependent stability of oxPL in culture media under different serum conditions 40

Figure 6: Protein pattern of apoptotic blebs 41

Figure 7: Effects of oxPL on aSMase activity and aSMase mediated apoptosis 43

CHAPTER 3

UPTAKE AND PROTEIN TARGETING OF FLUORESCENT OXIDIZED PHOSPHOLIPIDS IN CULTURED RAW 264.7 MACROPHAGES

Figure 1: Chemical structures of oxPL and their fluorescent analogs 70

Figure 2: Characterization of molecular and supramolecular carriers of BY-POVPE 72

Figure 3: Uptake of oxPL by RAW 264.7 macrophages from different carriers 74

Figure 4: Transfer of BY-POVPCE between lipid donors 77

Figure 5: Covalent interaction of POVPC with protein and lipid targets 78

Figure 6: Protein targets of fluorescent BY-POVPE in RAW 264.7 macrophages 80

Table 1: Protein targets of BY-POVPE in total RAW 264.7 lysates 82

Table 2: Protein targets of BY-POVPE in total membrane fraction 83

Figure 7: Exchange of BY-POVPE between lipid-protein surfaces 89

CHAPTER 1

SUMMARY

1. SUMMARY AND AIMS

The uptake of oxidized low-density lipoprotein (oxLDL) by the macrophages of the vascular wall and the accumulation of apoptotic cells in atherosclerotic lesions are hallmarks of atherosclerosis (1). The harmful effects of oxLDL are not only associated with lipid accumulation in macrophages and other vascular cells. They are also mediated by the intrinsic toxicity of a great variety of lipid oxidation products that are generated in low-density lipoprotein (LDL) under the conditions of oxidative stress. These compounds comprise oxidized sterols, oxidized fatty acid derivatives and oxidized glycerophospholipids. They have been found in plasma LDL and in lipid deposits as well as in lipoproteins isolated from atherosclerotic plaques (2). The main phospholipid species in the surface of native LDL contain linoleic and to a lesser extent arachidonic acid in position *sn*-2 of glycerol (3). Under the influence of reactive oxygen species, a great variety of products is formed, such as oxidized phospholipids (oxPL), which may contain a modified long-chain carboxylic acid or a truncated acyl residue with a polar functional group at its ω-end. Typical derivatives of truncated phospholipids are the chemically reactive aldehydo-phospholipids POVPC and Poxno-PC (from arachidonoyl- and linoleoyl phospholipids, respectively) and the carboxy-phospholipids PGPC and Paze-PC (also from arachidonoyl- and linoleoyl phospholipid, respectively). These compounds show the same structural features except for the functional group at the ω-end of the *sn*-2 chain. In PGPC and Paze-PC, this is a carboxylate residue which renders the entire molecule negatively charged. POVPC and Poxno-PC contain an aldehyde function which is less polar. However, it is chemically reactive and can undergo Schiff base formation with amino groups of proteins and aminophospholipids (4). The truncated phospholipids contain only a

single hydrophobic long-chain fatty acid in position *sn*-1 attaching the amphiphile to the hydrophobic domain of the bilayer. The *sn*-2 acyl residue is short and polar. Therefore, these compounds show similar (supra)molecular features compared with other biologically active phospholipids, namely lysolecithin and platelet activating factor (PAF) (2).

Sustained exposure to minimally modified LDL (mmLDL) induces apoptosis in macrophages, which is mediated by the activation of an acid sphingomyelinase (aSMase) generating the apoptotic lipid messenger ceramide (5). mmLDL can be obtained by mild oxidation of LDL *in vitro* and is perhaps a reliable model for the oxidized LDL formed *in vivo*. It is characterized by a significant fraction of lipid oxidation products and a low degree of protein modification (6). As a consequence its toxicity is largely due to its content of oxPL.

It was the aim of the first part of this doctoral thesis to find out whether and to what extent the apoptotic effects of the modified lipoprotein are mediated by truncated diacyl-phospholipids and the corresponding alkylacyl-phospholipids in cultured macrophages (Chapter 2). For this purpose, we used chemically defined PGPC and POVPC as well as their 1-O-hexadecyl analogs and determined their toxicity in the macrophage-like cell line RAW 264.7 and bone marrow-derived macrophages (BMM). Here we provide evidence that both oxidized phospholipids induce apoptosis in cultured macrophages. The tendencies of PGPC and POVPC to induce apoptosis were the same in both cell types, the bone marrow-derived cells being slightly more susceptible to phospholipid toxicity than the RAW 264.7 cells. POVPC rapidly activated aSMase in cultured RAW 264.7 macrophages. If the expression of aSMase was abolished by a specific inhibitor, the cells became more resistant to POVPC-induced apoptosis, showing that the activity of this enzyme is causally linked to

POVPC-induced toxicity in macrophages. PGPC showed a small inhibitory effect on aSMase. Preliminary data from our group support the assumption that the latter oxPL interferes with the enzymes of *de novo* ceramide synthesis localizing to intracellular membranes, whereas aSMase is likely to generate ceramide in the plasma membrane.

In addition to diacylglycerophospholipids (mainly phosphatidylcholine), LDL also contains small amounts of alk(en)yl-acyl-analogs (7). Animal and human cell membranes, except for the liver, contain large amounts of this phospholipid subclass. Most alk(en)ylacyl phospholipid species (mainly containing phosphocholine- and ethanolamine head groups) also contain polyunsaturated fatty acyl chains in position *sn*-2 of glycerol and therefore are subject to modification by reactive oxygen species, too (7). We found that the alkylacyl analogs of PGPC and POVPC are even more potent inducers of macrophage apoptosis than their diacyl counterparts. The same effects were also observed in cultured vascular smooth muscle cells (unpublished). Currently, we do not know the reason for the higher ether lipid toxicities, which may be due to differences in biochemical stability and biophysical properties. The *sn*-1 alkylether bond is resistant to hydrolytic cleavage and thus increases biochemical stability of the lipid molecule. From biophysical studies it is known that alkylacyl phospholipids are more densely packed and increase the tendency of the membrane or some membrane areas to adopt nonbilayer lipid phases leading to membrane destabilization and alterations of membrane-associated enzyme functions (8,9).

The second part of this doctoral thesis was devoted to the cellular uptake and the primary molecular targets of the oxidized phosphatidylcholines (Chapter 3). For this purpose, we used the BODIPY-labeled (BY) ethanolamine phospholipids BY- PGPE and BY- POVPE, as fluorescently labeled analogs of PGPC and POVPC respectively, carrying a polar BY- fluorophore linked to the polar lipid head groups (10). These

compounds were used for visualization of lipids in live cells and lipid-protein complexes in acrylamide or agarose gels. In a previous study, we have provided evidence that they are reliable model compounds of their unlabeled counterparts (10). We prepared and characterized two physiologically relevant donors containing the fluorescent lipid analogs and investigated the transfer of the labeled lipids from these systems to cultured macrophages using fluorescence microscopy. Conversely, we studied lipid transfer between the individual donors and the back-transfer of the lipids from the cells to the donors. Donor systems for our *in vitro* studies were defined complexes of the fluorescent lipids with albumin and LDL as well as aqueous lipid dispersions as reference systems. BY-PGPE and BY-POVPE are taken up into RAW 264.7 in a very different manner. BY-PGPE is quickly internalized from aqueous suspensions and albumin complexes. The fluorescence intensity inside the cells was significantly lower if labeled LDL was the lipid donor. This lipoprotein contains PAF-acetylhydrolase which also catalyzes the degradation of short-chain oxPL and reduces the stability of the oxidized lipid (11). BY-POVPE almost entirely localizes to the cell surface (colocalization with a plasma membrane-specific dye), due to Schiff base formation with membrane proteins and aminophospholipids. The lipid-protein complexes could be stabilized by chemical reduction and identified as putative primary targets of the phospholipid aldehyde (see below). In summary, lipid uptake does not depend on the donor system. The same cellular fluorescence patterns were obtained if oxPL were released to the cells from pure lipid dispersions, lipid-albumin complexes or lipid-loaded LDL. Despite the fact that the lipid aldehyde BY-POVPE is firmly bound to LDL and albumin, it is released from these carriers to the phospholipids and proteins of the cell plasma membrane suggesting high reversibility of Schiff base formation. BY-POVPE can be transferred from labeled LDL to unlabeled albumin in a concentration-dependent manner. Release of BY-POVPE from LDL is significantly

decreased after reduction of the Schiff bases leading to the formation of stable amine bonds. If cells labeled with BY-POVPE were incubated with unlabeled albumin, the same phenomenon was observed. The partitioning of the aldehydo-phospholipid between the different biological surfaces can be explained by the pK values of aliphatic Schiff bases around the physiological pH (12). Under these conditions, a significant fraction of the imines in the protein- and lipid-complexes of BY-POVPE is protonated and therefore prone to nucleophilic attack by other amines in the sample.

We isolated and identified the protein targets of BY-POVPE in cultured RAW 264.7 macrophages, which are expected to form covalent Schiff base adducts. Because the imine complexes are unstable, they were stabilized before isolation and separation by chemical reduction leading to the formation of the stable amines. We used a proteome approach to identify the lipid binding proteins in total cell lysates as well as in the total membrane fractions. The fluorescence patterns, reflecting the labeled protein targets, are much less complex than the total protein patterns detected after unspecific protein staining. Obviously, protein targeting by the oxPL is selective rather than random. This effect may be due to the different pK values of differently exposed amino groups and steric constraints as a consequence of different lipid-protein and protein-protein interactions in the membrane. The protein targets of BY-POVPE were identified by MS/ MS analysis. They are involved in membrane transport (e.g. VDAC), stress response (e.g heat shock proteins), apoptosis (e.g. Cathepsin D, caspases) and lipid metabolism (e.g. N-acyl-sphingosine hydrolase).

In summary, we have shown that fluorescent analogs of PGPC and POVPC are easily taken up into macrophages irrespective of the lipid presentation. Whereas POVPC is initially scavenged by covalent reaction with the components of the plasma membrane, PGPC is quickly internalized. Despite the covalent binding to its lipid and protein targets, POVPC is freely exchangeable between membranes and (lipo-)

protein surfaces. As a consequence, this lipid represents a toxic compound which is active not only at the site of its formation, but also in cells far distant from areas of oxidative stress. The identification of the potential POVPC protein targets supports the assumption that POVPC interacts with multiple sites and not only with the traditional specific receptors.

2. REFERENCE LIST

1. Glass, C. K. and Witztum, J. L. (2001) *Cell* **104,** 503-516

2. Fruhwirth, G. O., Loidl, A., and Hermetter, A. (2007) *Biochim.Biophys.Acta* **1772,** 718-736

3. Mertens, A. and Holvoet, P. (2001) *FASEB J.* **15,** 2073-2084

4. Friedman, P., Horkko, S., Steinberg, D., Witztum, J. L., and Dennis, E. A. (2002) *J.Biol.Chem.* **277,** 7010-7020

5. Deigner, H. P., Claus, R., Bonaterra, G. A., Gehrke, C., Bibak, N., Blaess, M., Cantz, M., Metz, J., and Kinscherf, R. (2001) *FASEB J.* **15,** 807-814

6. Salvayre, R., Auge, N., Benoist, H., and Negre-Salvayre, A. (2002) *Biochim.Biophys.Acta* **1585,** 213-221

7. Marathe, G. K., Davies, S. S., Harrison, K. A., Silva, A. R., Murphy, R. C., Castro-Faria-Neto, H., Prescott, S. M., Zimmerman, G. A., and McIntyre, T. M. (1999) *J.Biol.Chem.* **274,** 28395-28404

8. Smaby, J. M., Hermetter, A., Schmid, P. C., Paltauf, F., and Brockman, H. L. (1983) *Biochemistry* **22,** 5808-5813

9. Sommer, A., Paltauf, F., and Hermetter, A. (1990) *Biochemistry* **29,** 11134-11140

10. Moumtzi, A., Trenker, M., Flicker, K., Zenzmaier, E., Saf, R., and Hermetter, A. (2007) *J.Lipid Res.* **48,** 565-582

11. Chen, C. H. (2004) *Curr.Opin.Lipidol.* **15,** 337-341

12. Sheves, M., Albeck, A., Friedman, N., and Ottolenghi, M. (1986) *Proc.Natl.Acad.Sci.U.S.A* **83,** 3262-3266

CHAPTER 2

TOXICITY OF OXIDIZED PHOSPHOLIPIDS IN CULTURED MACROPHAGES

U. Stemmer[1], S. Dunai[1], D. Koller[1], G. Pürstinger[1], E. Zenzmaier[1], E. Aflaki[2], D. Kratky[2], and A. Hermetter[1]

[1] Institute of Biochemistry, Graz University of Technology, A-8010 Graz, Austria

[2] Institute of Molecular Biology and Biochemistry, Medical University of Graz, A-8010 Graz, Austria

1. ABSTRACT

The interactions of oxidized low-density lipoprotein and macrophages are hallmarks in the development of atherosclerosis. The biological activities of the modified particle in these cells are due to both, the content of lipid oxidation products and apolipoprotein modification by oxidized phospholipids. It was the aim of this study to determine the role of short-chain oxidized phospholipids as compounds of modified low-density lipoprotein (LDL) in cultured macrophages. For this purpose we studied the effects of the following oxidized phospholipids on cell viability and apoptosis: 1-palmitoyl-2-glutaroyl-*sn*-glycero-3-phosphocholine (PGPC), 1-palmitoyl-2-(5-oxovaleroyl)-*sn*-glycero-3-phosphocholine (POVPC) and oxidized dialkyl phospholipids including, 1-O-hexadecyl-2-glutaroyl-*sn*-glycero-3-phosphocholine (E-PGPC) and 1-O-hexadecyl-2-(5-oxovaleroyl)-*sn*-glycero-3-phosphocholine (E-POVPC). We found that these compounds induced apoptosis in RAW 264.7 and bone marrow-derived macrophages. The *sn*-2 carboxyacyl lipid PGPC was more toxic than POVPC, which carries a reactive aldehyde function in position *sn*-2 of glycerol. The alkyl phospholipids (E-PGPC and E-POVPC) were even more active than the respective diacyl analogs. Apoptosis induced by POVPC and its alkylether derivative could be causally linked to the fast activation of an acid sphingomyelinase, generating the apoptotic second messenger ceramide. In contrast, PGPC and its ether analog hardly showed any effect on this enzyme pointing to an entirely different mechanism of lipid toxicity. The higher toxicity of PGPC is underscored by more efficient membrane blebbing from apoptotic cells. In addition, the protein pattern of PGPC-induced microparticles is different from the vesicles generated by POPVC. In summary our data show that oxidized phospholipids induce apoptosis in cultured

macrophages. However, the mechanism of lipid toxicity largely depended on the structural features of the oxidized *sn*-2 chain.

2. INTRODUCTION

Macrophages are prominent in atherosclerotic lesions. Within the fraction of lesional macrophages in a proliferating state, a subset becomes apoptotic or necrotic (1). Studies of advanced atherosclerotic lesions revealed a strong correlation between macrophage cell death and the incidence of plaque rupture associated with acute vascular events (2). A very early and presumably initiating event in atherogenesis is the focal retention of modified low-density lipoprotein (e.g. oxidized (ox)LDL) in the subendothelial space. Some of the particles that accumulate in the macrophages of atherosclerotic lesions are thought to be oxidized either prior to uptake into the arterial wall or subsequently due to intracellular chemical processes, e.g. free radical-mediated modifications. The modified lipoprotein particles can inhibit or induce cell death, depending on the extent of lipoprotein oxidation and lipoprotein dose (3). In cell culture, apoptosis of macrophages can be initiated by minimally (e.g. by Fe^{2+}) modified LDL (mmLDL), in which the lipids but not the apolipoproteins are oxidized (4). From this observation it can be inferred that the oxidized lipids are largely responsible for the toxic effects of this particle. It has been shown that the toxicity of oxidized phospholipids (oxPL) is increased in cells undergoing ER stress due to other (lipo)toxic agents (5).

mmLDL stimulates acid sphingomyelinase (aSMase) activity within minutes, leading to the formation of the second messenger ceramide which mediates the apoptotic signal in vascular cells including macrophages, endothelial cells and vascular smooth muscle cells (3,6-8). Ceramide is a second messenger that activates several apoptotic signalling pathways. In vascular smooth muscle cells, the stress-induced

protein kinases JNK and p38 MAPK have been identified as such components of cells exposed to mmLDL (7).

It has already been shown that ceramide-mediated apoptosis can also be induced in these cells by oxPL (7). These compounds are generated from polyunsaturated phosphatidylcholines in LDL under the conditions of oxidative stress. Among a plethora of lipid oxidation products, oxPL, such as 1-palmitoyl-2-(5-oxovaleroyl)-*sn*-glycero-3-phosphocholine (POVPC) and 1-palmitoyl-2-glutaroyl-*sn*-glycero-3-phosphocholine (PGPC), are present in mmLDL (9). They show a high capacity to induce apoptosis in vascular smooth cells (10) and macrophages, especially if the latter cells sense ER stress (5). Both compounds are oxidation products of phosphatidylcholines containing arachidonic acid in the *sn*-2 position of the glycerol. They are characterized by a short fatty acyl chain in position *sn*-2 and a hydrophobic, long-chain, fatty acid in the *sn*-1 position of glycerol. In addition to diacyl-phospholipids, LDL contains the 1-O-alk(en)yl-2-acyl-analogs which are also modified by radical-mediated oxidation (11). The truncated diacyl and alk(en)ylacyl phospholipids share similar structural features with two highly bioactive lipoprotein and membrane components, namely platelet-activating factor (PAF) and lysolecithin (12,13). They are more polar than unmodified membrane or lipoprotein phospholipids. Since they contain only one long hydrophobic *sn*-1 acyl or alkyl chain, they exchange easily between tissues, cells, and lipoproteins (Stemmer et al., submitted, see Chapter 3).

Exposure of vascular smooth muscle cells to POVPC and to a lesser extent PGPC elicited fast activation of an aSMase in these cells (7,10) pointing to an effect on the protein level. Although both oxPL lead to the same endpoint (apoptosis), their mechanisms of toxicity are likely different. The *sn*-2-aldehydoacyl phospholipid

POVPC chemically interacts with the free amino groups of proteins or phospholipids via Schiff base formation (14). After cellular uptake, most of the lipid is retained in the cell surface. In contrast, PGPC containing a carboxyacyl residue in position *sn*-2 can only physically interact with the molecules in its close vicinity and is rapidly internalized by the cells (Stemmer et al., submitted, see Chapter 3).

It was the aim of this study to find out whether and to what extent the apoptotic effects of mmLDL are mediated by truncated diacylphospholipids and the corresponding alkylacyl phospholipids in cultured macrophages. For this purpose, we used chemically defined PGPC and POVPC as well as their 1-O-hexadecyl analogs and determined their toxicity in the macrophage-like cell line RAW 264.7 and bone marrow-derived macrophages (BMM). Although the latter cells proved to be more sensitive towards the oxPL, both cell types showed the same tendencies. The four lipids under investigation mainly induced apoptosis in these cells. PGPC was more toxic than POVPC. The alkylacyl phospholipids are even more active than the respective diacyl analogs. Apoptosis induced by POVPC and its alkylether derivative could be causally linked to the activity of aSMase. The more toxic lipids PGPC and its ether analog hardly showed any effect on this enzyme pointing to an entirely different mechanism of lipid toxicity. The higher toxicity of PGPC is underscored by more efficient membrane blebbing from the apoptotic cells producing lots of lipid particles that in turn contain high amounts of oxPL that propagate the toxic phospholipids effects to other cells (and organs).

3. MATERIALS AND METHODS

3.1 MATERIALS

Oxidized phospholipids (PGPC and POVPC) were synthesized in our laboratory as previously described (15). 1-O-alkyl-ether analogs were prepared starting from 1-O-hexadecyl-sn-glycero-3-phosphocholine and glutaric acid anhydride as described for the acylation of the 1-acyl-phospholipid (15). 1-palmitoyl-2-oleoyl-*sn*-glycero-3-phosphocholine (POPC) was synthesized according to the procedure of Hermetter et al. (16). 1-palmitoyl-*sn*-glycero-3-phosphocholine (PLPC) was purchased from Bachem (Bubendorf, Switzerland). Chemicals for gel electrophoresis were from BioRad Laboratories (Hercules, CA), unless otherwise noted. NB19 was kindly provided by Dr. Hans-Peter Deigner (Frauenhofer EXIM/CEOS, Rostock, Germany). Organic solvents and all other chemicals were purchased from Carl Roth (Karlsruhe, Germany), Sigma-Aldrich (Steinheim, Germany) or Merck (Darmstadt, Germany). Tissue culture materials were obtained from Sarstedt (Nürmbrecht, Germany) or Greiner (Kremsmünster, Austria). Dulbecco's modified Eagle medium (DMEM, 4,5 g/l Glucose) with and without phenol red and heat-inactivated fetal bovine serum, Vybrant® MTT Cell proliferation Assay kit (V-13154), Vybrant® apoptosis assay kit#2 (V-132451), F4/80 antibody and matching isotype control and staurosporine were from Invitrogen (Leek, Netherlands). PBS and cell culture supplements were obtained from PAA (Linz, Austria), unless otherwise indicated. "Fluids" for flow cytometry, FACS tubes und cells strainers were from BD bioscience (Heidelberg, Germany).

3.2 CELL CULTURE

The macrophage-like cell line RAW 264.7 (ATCC No. TIB-71, American Type Culture collection, Rockville, MD, USA) was routinely grown in DMEM (4,5 g/l glucose, 25 mM

HEPES, 4 mM L-glutamine, without sodium pyruvate) supplemented with 10% heat-inactivated fetal calf serum (FCS) and 100 U/ml penicillin/streptomycin at 37°C in humidified CO_2 (5%) atmosphere. Bone marrow-derived macrophages (BMM) were isolated according to a slightly modified standard protocol provided by Invitrogen (Leek, Netherlands). Femur and tibia of C57Bl/6 mice were separated and placed on ice in sterile PBS. The excess muscle was removed and the ends of the bones were cut off on both sides. Cells were washed out with a 26-G needle attached to a sterile syringe, filled with 3 ml DMEM (4,5 g/l D-glucose, 4mM glutamine, 110 mg/l sodium pyruvate) and transferred via a cell strainer into a 50 ml falcon tube. Subsequently the cell suspension was centrifuged at 500- 800 g for 15 minutes and the supernatant was discarded. The cell pellet was carefully resuspended in DMEM supplemented with 10% LPDS and 500 U/ml penicillin/streptomycin and transferred into a culture flask (175 cm^2 / 3 mice) followed by incubation at 37°C in a humified 5% CO_2 atmosphere for 24 h. Nonadherent cells were removed the next day, counted and resuspended in DMEM containing 10 ng/ml MCSF (R&D Systems, Minneapolis, USA). Cells were seeded in 96 well plates (10^6 cell/100 µl) for the MTT assay or in 24 well plates ($4*10^6$ cells/ 500 µl) for apoptosis assay. After 3 and 5 days the medium was replaced with fresh, supplemented DMEM containing 10 ng/ml MCSF.

3.3 ASSESSMENT OF BMM DIFFERENTIATION

Monocyte differentiation was proven with rat anti mouse F4/80- R-PE antibody and rat IgG2a R-PE isotype control using flow cytometry. The former monoclonal antibody reacts with the mouse F4/80 antigen which is a macrophage-specific glycoprotein. Monocyte differentiation was analyzed on the first and seventh day using RAW 264.7 macrophages as a reference. 10^6 cells were transferred to a FACS tube and centrifuged at 2000 g for 3 minutes. Cells were resuspended in PBS containing 2 mg/ml glucose.

0,25 µg of the antibody or the isotype control were added followed by incubation at room temperature in the dark for 15 minutes. Stained samples were analyzed using a FACS Calibur instrument (BD Bioscience, Heidelberg, Germany). The red fluorescence emission was measured above 575 nm upon excitation with a 488 nm laser. The percentage of differentiated cells was calculated using WinMDI 2.8 software. A content of 90-95% differentiated cells was considered as appropriate for further experiments.

3.4 INCUBATION OF CELLS WITH oxPL

Aqueous lipid dispersions containing various µM concentration of oxPL, POPC or PLPC (0-200 µ,M) were prepared using the ethanol injection method (17). Cells were incubated with lipid dispersions in PBS or culture media without phenol red at various serum concentrations (0-10%, v/v). The final ethanol concentration in the incubation mixtures did not exceed 1% (v/v) of total volume. Culture media or PBS with this ethanol concentration was routinely used as controls.

3.5 MTT VIABILITY ASSAY

To determine the cytotoxic effect of oxPL in macrophages Vybrant® MTT Cell proliferation Assay kit was used according to the manufacturer's recommendations. The MTT assay involves the conversion of the water soluble MTT (3-(4,5-dimethylthiazol-2-yl)-2,5-diphenyltetrazolium bromide) to an insoluble formazan by viable cells. The formazan is solubilized, and its concentration is determined from the optical density at 570- 600 nm. The protocol was optimized for RAW 264.7 and BMM according to cell number, MTT concentration and incubation times. In brief, $1{,}25*10^5$ RAW 264.7 cells or 10^6 monocytes were seeded in 96 well plates in culture medium with varying FCS concentrations. Monocytes were differentiated before incubation as described above. RAW 264.7 cells were left in the wells for 2-3 h to ensure attachment to the substratum. The medium was removed and the lipid dispersions or control substances (1% v/v

EtOH, 2,5 mM H_2O_2, 1 µM staurosporin) in PBS or culture medium were added. After incubation, the lipid-containing medium was replaced by 100 µl fresh medium and 10 µl MTT (1 mg/ml) solution were added prior to incubation at 37°C in a humified 5% CO_2 atmosphere for 2 h. Subsequently, 100 µl 10% (w/v) SDS in 0,01% (v/v) HCl was added. The cells were incubated under the same conditions for 4 h. The mixture was solubilized to homogeneity and optical density was measured at 595 nm using an Anthos plate reader driven by WinRead 2.3 software.

3.6 FLOW CYTOMETRIC APOPTOSIS ASSAY

Samples were prepared as described for the MTT assay (see above), except for the cell number and plate format. Specifically, 6,5 *10^5 RAW 264.7 or 4*10^6 monocytes were initially seeded in a 24 well plate (volume 3 ml). Cells were harvested by scraping and washed with cold PBS containing 2 mg/ml glucose prior to resuspension in Annexin V binding buffer. 3*10^5 cells/ 100 µl were transferred in a FACS tube. 5 µl AlexaFluor®488 Annexin V and 5,5 µl Propidium iodide (PI; 1 mg/ml) were added and allowed to incubate at room temperature in the dark for 15 minutes. Prior to FACS measurement, samples were diluted in 400 µl PBS containing 2 mg/ml glucose, gently mixed and kept on ice until analysis. Stained samples were then analyzed using a FACS Calibur flow cytometer (BD Bioscience, Heidelberg, Germany). The green and red fluorescence were measured at 530 nm and 575 nm, respectively (excitation: 488 nm laser). Populations were separated into four groups. Apoptotic cells were stained by green fluorescent AlexaFluor®488 AnnexinV, which labels phosphatidylserine on the cell surface; necrotic cells were only stained with PI, live cells were unstained. Double-stained cells can be considered as late apoptotic or early necrotic. They were determined separately. The percentage of apoptotic cells was calculated using WinMDI 2.8 software package. Apoptotic effects of 1-O-alkylether lipids and NB19 were

compared with PGPC and POVPC-induced apoptosis under the same conditions except for the cell number. For these experiments, cells were left overnight in the multi-well plate and as a consequence, cell numbers were twice as high. Cells were pre-incubated with 10 µM NB19 in order to determine the effect of aSMase on apoptosis. NB19 was dissolved in EtOH before addition to the culture medium (10 nmol NB19/ml) for 30 minutes. The final ethanol concentrations in the incubation mixtures did not exceed 1% (v/v) of total volume.

3.7 MORPHOLOGICAL STUDIES

Monolayer cultures of RAW 264.7 cells were grown to 60-80% confluence in chamber slides (Nunc, Nalgene, Rochester, USA). Cells were incubated with aqueous dispersions of oxPLs or reference compounds (1% v/v EtOH, 2,5 mM H_2O_2, 1 µM Staurosporin, PLPC) in DMEM without phenol red under low serum conditions (0,1% FCS) at the indicated concentration over various incubation times. After incubation, cells were carefully rinsed with PBS and observed with an Axiovert 35 inverted microscope equipped with a CCD camera, driven by AxioVision software package (Carl Zeiss, Germany).

3.8 PROTEINS OF APOPTOTIC BLEBS

RAW 264.7 macrophages were grown to 80% confluence in Petri-dishes (10 cm diameter) and incubated with an aqueous dispersion of 50 µM oxPL or 1%(v/v) EtOH in DMEM under low serum conditions (0,1% FCS) for 18 h. Membrane vesicles and apoptotic blebs were harvested as described previously (18). Briefly, culture supernatants containing the membrane vesicles were isolated and cleared from debris and detached cells by centrifugation at 500 g for 10 minutes. Blebs were isolated by ultracentrifugation (100000 g for 90 minutes at 4°C). The pellet was washed and resuspended in 30 µl PBS prior to protein determination using a plate assay according

to the method of Bradford (19). 20 µl of pellet suspensions or supernatants (20 µg protein) were separated by SDS gel electrophoresis (4,5% stacking gel, 10% resolving gel) as previously described (20). Total proteins were stained with Sypro Ruby™ and detected using a BioRad laser scanner (Ex. 488 nm, Em. 530/30 nm).

3.9 TIME-DEPENDENT STABILITY OF oxPL

Stability of oxPL in serum-containing media was determined as previously described (10). Solvent was removed from 100 µM oxPL under a stream of nitrogen. 200 µl DMEM containing 10% or 0,1% FCS were added followed by incubation under shaking (575 rpm) for 2, 4, 6 or 20 h. After incubation, phospholipids were extracted with chloroform/methanol 2/1 (v/v) at room temperature. The organic phase was removed under gentle stream of nitrogen. The lipids were then dissolved in chloroform/methanol 2/1 (v/v) and analyzed by thin-layer chromatography. The mobile phase was chloroform/methanol/acetone/glacial acetic acid/water 20/40/10/10/10 (v/v/v/v/v) for PGPC and E-PGPC and chloroform/methanol/water 50/30/10 (v/v/v) for POVPC and E-POVPC, respectively. Lipid spots were detected with molybdenum blue reagent which specifically stains phospholipids (21).

3.10 ACID SPHINGOMYELINASE ACTIVITY

Cultured RAW 264.7 macrophages were harvested and counted using Countess System (Invitrogen). $1{,}3*10^6$ cells were plated in 6 well plates followed by incubation at 37°C in a humified 5% CO_2 atmosphere for 24 h. Subsequently, cells were washed with DMEM containing 0,1% FCS. OxPL-containing media was prepared by adding ethanolic lipid solutions to DMEM at room temperature under stirring. Cells were incubated with ethanolic solutions of 25 µM oxPL in DMEM at 37°C in a humified 5% CO_2 atmosphere for 0-15 minutes. Control cells were incubated with 1% ethanol (v/v) in DMEM under the same conditions and used as control cell populations. After the incubation, all steps

were carried out at 4°C. Cells were scraped into 1 ml PBS and the cell suspensions were transferred into 15 ml falcon tubes followed by centrifugation at 1500 rpm for 10 minutes. The supernatant was discarded and the cell pellet was resuspended in 50 µl acid lysis buffer for the determination of aSMase activity as described previously (22). Briefly, protein concentration of the cell lysates was determined using a plate assay according to the method of Bradford (19) and aliquots containing 20 µg protein were incubated with NBD-sphingomyelin substrate as described (22). Substrate and product were separated using thin-layer chromatography (TLC). The fluorescent lipids were quantified with a CCD camera (Herolab, Vienna) (excitation wavelength: 365 nm) using EasyWin software.

3.11 STATISTICAL ANALYSIS

Results are expressed as means +/- standard deviation (SD). Two-tailed unpaired Student's t-test was used to determine the significance of the measured differences. A p-value ≤ 0,05 was considered significant.

4. RESULTS

The oxPL PGPC and POVPC are components of oxLDL which is causally involved in the onset and progression of atherosclerosis (23). We have already shown that the toxicity of oxLDL in cultured vascular smooth muscle cells is largely due to its oxPL components. PGPC, POVPC and oxLDL induce apoptosis in these cells, which is mediated by aSMase generating the second messenger ceramide (7). It was the aim of this study to find out whether and to what extent PGPC and POVPC (Figure 1) induce (programmed) cell death in macrophages, which is a hallmark in atherogenesis.

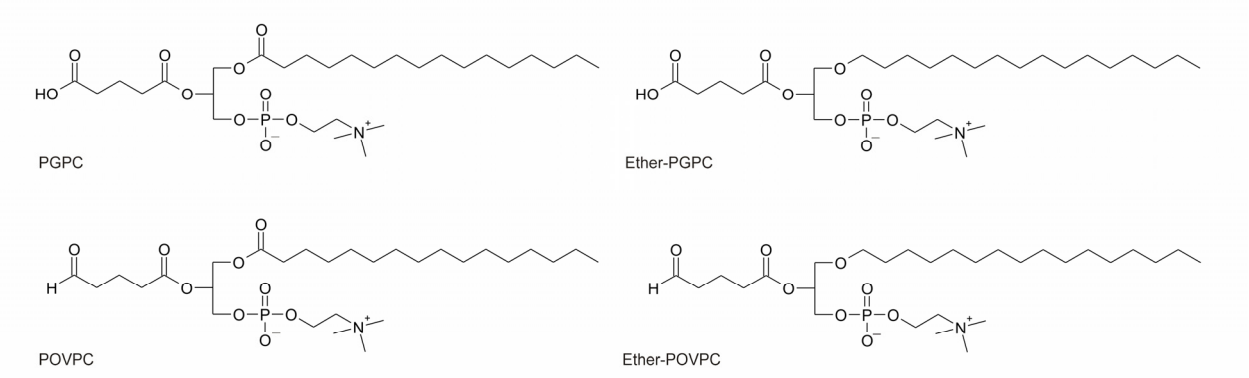

Figure 1: Chemical structures of oxidized phospholipids

PGPC: 1-palmitoyl-2-glutaroyl-*sn*-glycero-3-phosphocholine

Ether-PGPC: 1-O-hexadecyl-2-glutaroyl-*sn*-glycero-3-phosphocholine

POVPC: 1-palmitoyl-2-(5-oxovaleroyl)-*sn*-glycero-3-phosphocholine

Ether-POVPC: 1-O-hexadecyl-2-(5-oxovaleroyl)-*sn*-glycero-3-phosphocholine

For this purpose, we used the established RAW 264.7 macrophage-like cell line and cultured murine BMM. In a pre-screen, the effects of both oxPL on cell viability were studied using the photometric MTT assay (Figure 2). From the decrease in optical

density of the marker dye it can be concluded that both compounds decreased the viability of RAW 264.7 cells in a concentration- and for PGPC in time-dependent manner (Figure 2 A and B). PGPC was always more toxic than POVPC in these cells. Notably, the BMM were more sensitive towards the oxPL than the RAW 264.7 cells (Figure 2 C and D).

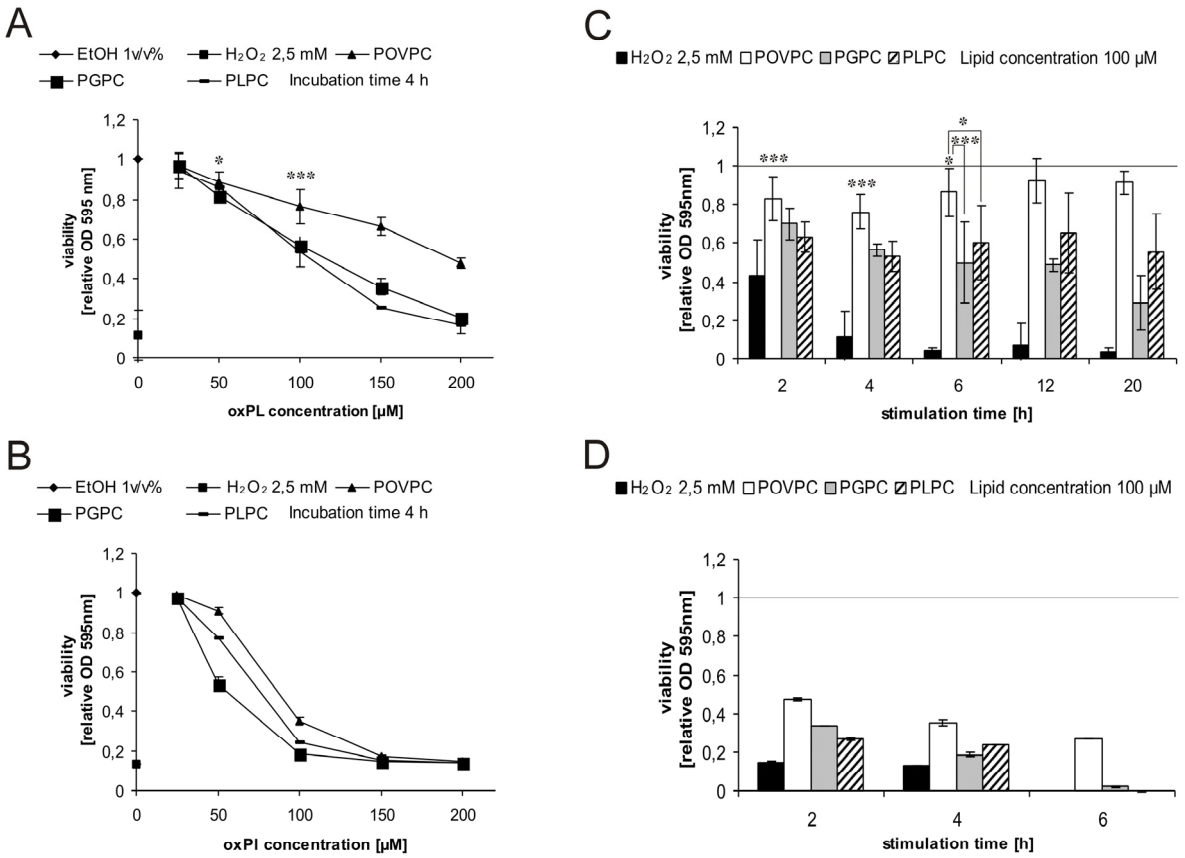

Figure 2: Effects of oxPL on viability of RAW 264.7 and BMM

RAW 264.7 cells (Panel A and B) and BMM (Panel C and D) were incubated with lipid dispersions in DMEM under low serum conditions (0,1 % FCS) depending on lipid concentration and incubation times. Cell viabilities were determined using the MTT assay described under materials and methods. Indicated values are relative viabilities (viability of control cells were set one). Results obtained with RAW 264.7 cells are means of 6 replicates out of three independent experiments. Results obtained with BMM (isolated and pooled from femurs and tibias of three or five mice, see materials and methods) are means of 4 replicates

out of two independent experiments. Significance was determined by Student's t-test (two tailed, unpaired) * p<0,05, *** p<0,005.

Lysophosphatidylcholine (PLPC) showed similar effects on viability as compared to PGPC (Figure 2). The former lipid and the oxPL show similar structural features since they contain only one long-chain fatty acyl residue in position *sn*-1 and a polar group in position *sn*-2 of glycerol. Since lysophosphatidylcholine is formed upon hydrolytic degradation of PGPC and POVPC (see also Figure 5), it can be expected that it contributes to the toxicities of these lipids to some extent, especially after long incubation times.

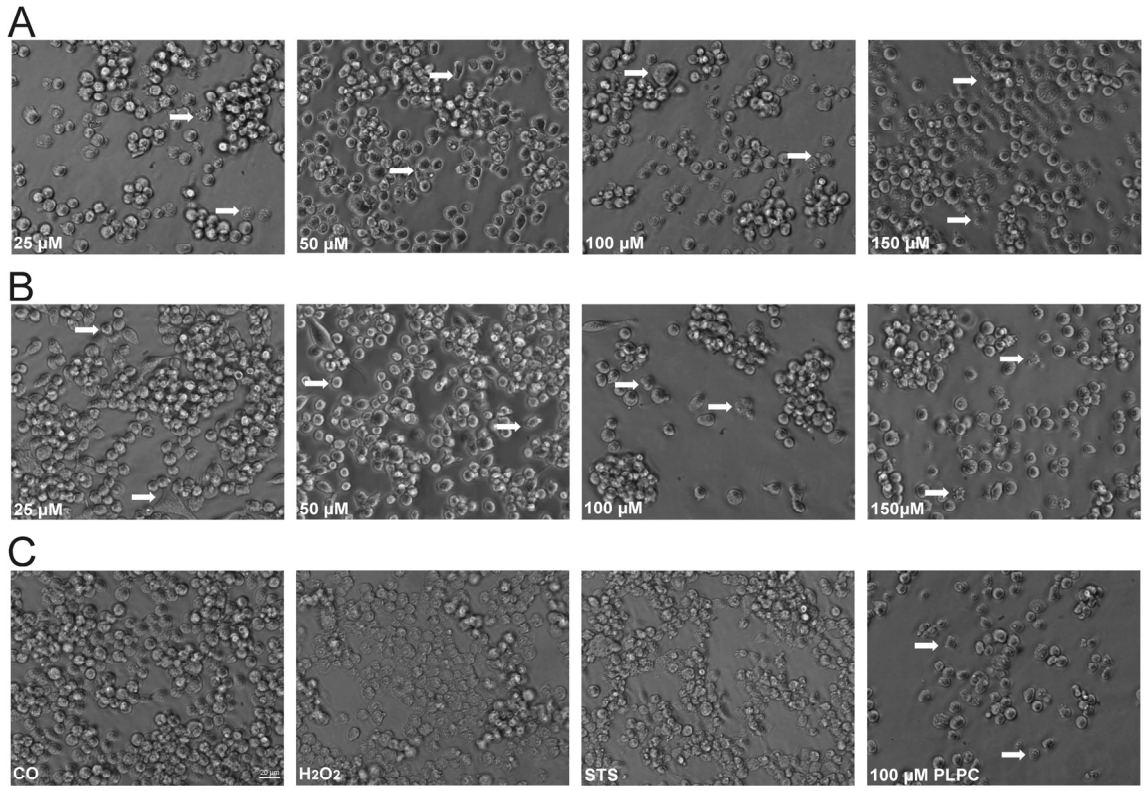

Figure 3: Morphological changes in RAW 264.7 macrophages

Photomicrographs (320 x magnification) of RAW 264.7 cells after incubation with POVPC (Panel A) and PGPC (Panel B) in DMEM containing 0,1% FCS for 4 h. Reference cells (Panel C) were incubated with 1 % v/v EtOH (Co), 2,5 mM H_2O_2 (necrosis) or 1 µM

staurosporin (STS; apoptosis) or lyso-PC (PLPC). Signs of cellular damage are cell detachment, morphological changes and membrane vesicle formation (indicated by arrows). Control cells (Co) showed no visible effect even upon prolonged incubation time (20 h).

Cell damage detected by the MTT assay is in line with the morphological changes that are seen under the microscope (Figure 3). Upon treatment with oxPL and lysophosphatidylcholine, RAW 264.7 cells show morphological changes such as rounding and shrinking and are eventually release from the solid substratum.

The detrimental effects of both oxPL on cell viability are associated with an increase in apoptosis. Programmed cell death under the influence of PGPC and POVPC was determined from cell staining with fluorescent Annexin V followed by FACS analysis. In addition, the capacity of the oxPL to induce necrosis was measured in the same experiment using PI as dye, staining the DNA in cells with permeabilized membranes. Staurosporine and hydrogen peroxide were used as control toxins to assess apoptosis and necrosis, respectively. PGPC and POVPC induced apoptosis in both cell types, PGPC being again more toxic than POVPC (Figure 4 A and B). Cells under the influence of either oxPL hardly showed any signs of necrosis (data not shown). The BMM were again more sensitive to the oxPL than the RAW 264.7 cells. We also studied apoptosis of both cell types under the influence of the 1-O-alkyl-2-acyl analogs of PGPC and POVPC (Figure 1). The respective compounds are oxidation products of ether choline phospholipids that are also found in LDL and cell membranes of animals and humans (24). The ether analogs of PGPC and POVPC elicited more severe apoptotic effects in RAW 264.7 cells than their diacyl counterparts, with the PGPC analog being more toxic than the POVPC analog (Figure 4 C). It is obvious that the toxicities of the diacyl and alkylacyl oxPL depend on the small structural difference in the oxidized *sn*-2 acyl chain. The (ether) POVPC

contains an aldehyde group which can react with the amino groups of phospholipids and proteins, whereas PGPC can only undergo physical interactions with the molecules in its close vicinity. As a consequence, cellular lipid uptake, membrane effects, signalling platforms and the outcome, cell death, are different.

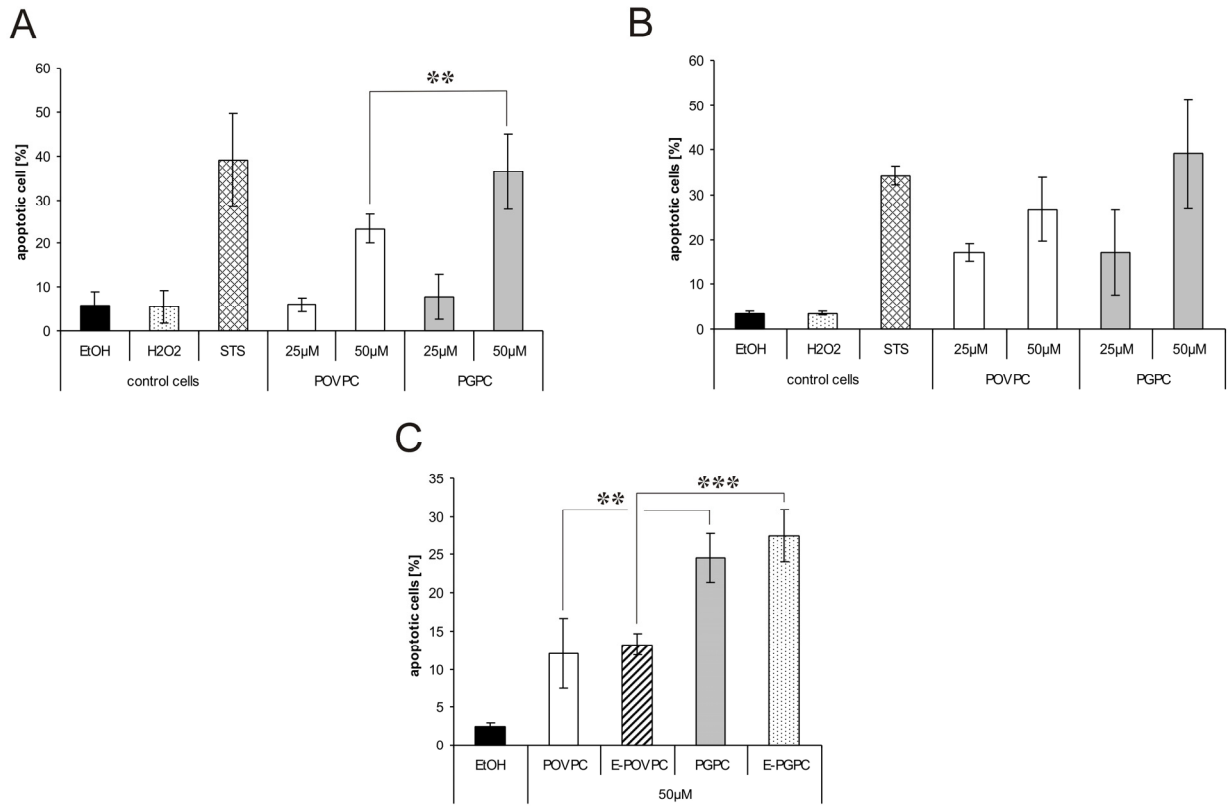

Figure 4: Apoptotic effects of oxPL in RAW 264.7 and BMM

Cells were incubated with the indicated concentrations of oxPLs in media under low serum conditions (0,1% FCS) for 4 h and analyzed by flow cytometry (see materials and methods). The fraction of apoptotic cells was determined from Annexin V staining of externalized phosphatidylserin. Control cells were incubated with 1% v/v Ethanol (EtOH). 2,5 mM H_2O_2 and 1µM staurosporin (STS) in the incubation media were used as reference agents inducing necrosis or apoptosis, respectively.

Panel A: 50 µM POVPC and PGPC induce apoptosis in RAW 264.7 macrophages. PGPC is a more potent inducer of cell death than POVPC under these conditions. Results are means of 6 replicates out of three independent experiments.

Panel B: 50 µM PGPC and POVPC induce apoptosis in BMM, which are slightly more sensitive to the oxPL. Results are means of 4 replicates of one pooled sample (BMM isolated and pooled from femurs and tibias of five mice, see materials and methods).

Panel C: 50 µM 1-O-alky ether analogs of PGPC and POVPC (E-PGPC and E-POVPC, respectively) induce apoptosis in RAW 264.7 macrophages.

All Results are expressed as means +/- SD. Significance was determined by Student's t-test (two tailed, unpaired) ** $p<0,01$, *** $p<0,005$.

Toxicity of oxPL in macrophages depends on lipid stability inside the cells and in the culture medium prior to cellular uptake. The cell viability and apoptosis experiments were performed under low serum conditions (0,1 % serum). In order to determine the stability of the oxPL, PGPC, POVPC and their ether analogs were incubated in the culture medium, followed by solvent extraction and TLC analysis. Under low serum conditions (0,1% FCS), POVPC (Figure 5 A) and ether-POVPC (Figure 5 B) were stable for two hours, whereas PGPC (Figure 5 A) and ether-PGPC (Figure 5 B) remained intact for 6h. This difference can help explain at least in part the higher toxicities of the PGPC versus the POVPC-derived lipids. Addition of 10 % serum to the culture medium efficiently catalyzed the hydrolysis of PGPC, POVPC (Figure 5 A) and their ether analogs (Figure 5 B) leading to the formation of lysophosphatidylcholine. After 2 h incubation, the entire amount of lipid has gone under these high serum conditions.

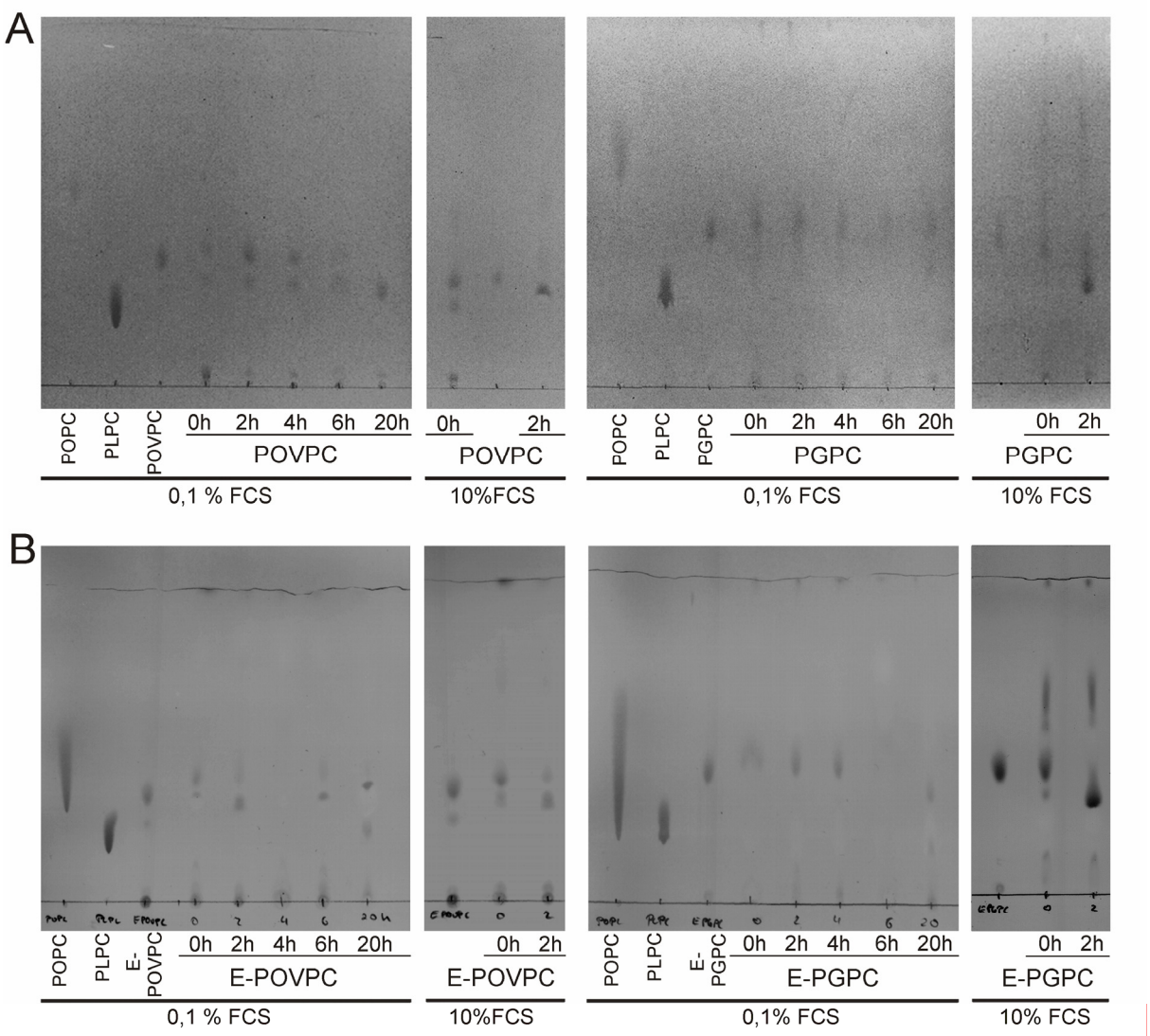

Figure 5: Time-dependent stability of oxPL in culture media under different serum conditions

OxPL were incubated in DMEM containing 0,1% or 10% serum for different times. Subsequently, lipids were isolated by solvent extraction and separated by thin layer chromatography. Mobile phase for PGPC (Rf= 0,43) and E-PGPC (Rf= 0,36), POPC (Rf >0,30) and PLPC (Rf=0,18) was chloroform/methanol/acetone/glacial acetic acid/water 20/40/10/10/10 (v/v/v/v/v). For POVPC (Rf= 0,35) and E-POVPC (Rf= 0,32), POPC (Rf >0,25) and PLPC (Rf=0,15) the mobile phase was chloroform/methanol/water 50/30/10 (v/v/v).

Under high serum conditions (10% FCS), POVPC and PGPC were converted to lysophospholipids. Under low serum conditions (0,1% FCS), PGPC was stable for at least 6 h, whereas POVPC started getting degraded immediately (Panel A). Notably, the major

amount of oxPL stayed intact during the incubation times used for cell experiments. The 1-O-alkyl ether analogs showed the same stabilities as their acyl counterparts (Panel B).

Apoptosis is associated with a series of profound changes in cellular structure and integrity. Membrane blebbing, the release of vesicular bodies (blebs) from the plasma membrane, is one of the hallmarks of this process (25,26). To measure the capacity of the oxPL to induce membrane blebbing in RAW 264.7 macrophages, cells were incubated with 50 µM PGPC or POVPC for 18 h (Figure 6). The vesicle pellets (P) were isolated from the supernatant (SN) by ultracentrifugation and analysed for their protein patterns and contents. The protein patterns of the apoptotic vesicles (P) slightly depended on the oxPL. However, the efficiency as determined from the protein amount in the membrane fraction (P) differed to a great extent depending on the lipid. Concerning the protein content we show that PGPC led to a much more pronounced release of apoptotic vesicles than POVPC.

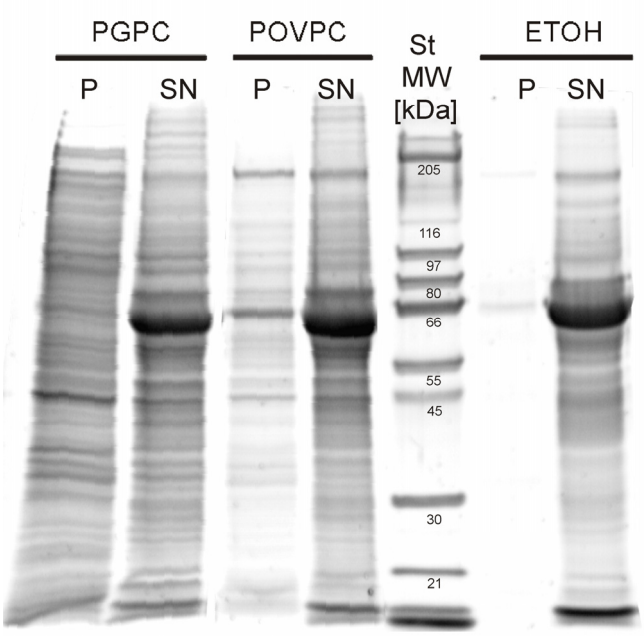

Figure 6: Protein pattern of apoptotic blebs

RAW 264.7 cells were incubated with 50 µM PGPC or POVPC or 1% (v/v) EtOH under low serum conditions (0,1% FCS) for 18 h. Membrane vesicles were isolated by

ultracentrifugation and resuspended in PBS. Pellets (P) and supernatants (SN) obtained after ultracentrifugation were separated by SDS PAGE as described in materials in methods section. Vesicles produced by POVPC and PGPC show slightly different protein patterns. More vesicles protein is released under the influence of PGPC.

In a previous study, we found that POVPC and, to a lesser extent, PGPC-induced apoptosis was mediated by the fast activation of an aSMase in cultured vascular smooth muscle cells (7). This enzyme generates ceramide from sphingomyelin, which propagates the apoptotic signal. The data presented in this work provide evidence that both oxPL induce apoptosis also in cultured macrophages, but the role of aSMase seems to be different in the latter cells. POVPC and ether-POVPC activate aSMase within minutes (Figure 7 A). The ether-POVPC stimulates the enzyme more efficiently. This result is in line with the higher toxicity of the ether-POVPC. FACS analysis of apoptosis in RAW 264.7 macrophages provided evidence that aSMase activity is directly linked to the toxicity of POVPC. Pre-incubation of the cells with an enzyme inhibitor (NB19) reduced the amount of apoptotic cells after exposure to the oxPL (Figure 7 B). PGPC and ether-PGPC show an opposite effect, they inhibit aSMase in macrophages (Figure 7 A). We have evidence that PGPC utilizes enzymes of the *de novo* pathway for ceramide production and signalling (unpublished). Interestingly, inhibition of aSMase expression by NB19 protects cells against the toxicity of PGPC (Figure 7 B), although there is no direct effect of the oxPL on enzyme activity. According to these data, there must be at least one indirect relationship between aSMase and PGPC-induced cell death. This open question will be subject to further clarification.

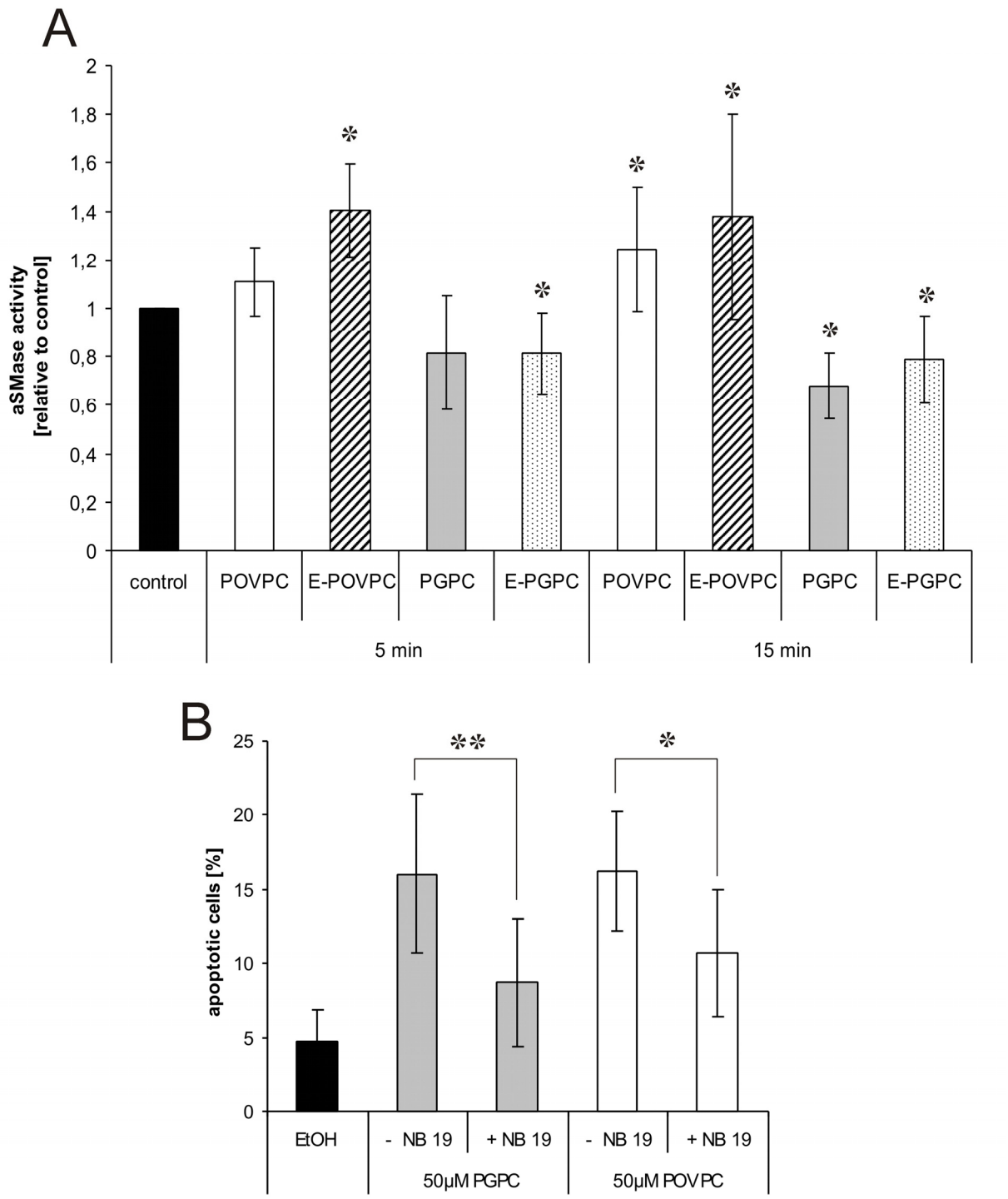

Figure 7: Effects of oxPL on aSMase activity and aSMase-mediated apoptosis

Panel A: RAW 264.7 cells were incubated with DMEM containing 25 µM of lipid or 1% v/v EtOH (control) for 5 or 15 minutes. Cells were harvested and lysed and sphingomyelinase activity was determined as described under materials and methods. POVPC and its 1-O-alkyl

ether analog (E-POVPC) increase aSMase activity within 5 minutes. PGPC and E-PGPE had a inhibitory effect on enzyme activity as compared to the control.

Panel B: RAW 264.7 cells were incubated with the 50 µM oxPLs in media under low serum conditions (0,1% FCS) for 4 h and analyzed by flow cytometry. The fraction of apoptotic cells was determined from Annexin V staining of externalized phosphatidylserin. Control cells were incubated with 1% v/v Etoh (EtOH) in the incubation media. Inhibition of aSMase with NB19 (10 nmol/ml) leads to significant decrease in apoptosis induced by POVPC and PGPC. NB19 alone had no effect on cell viability (data not shown). Results are means of 4 replicates out of 3 experiments.

Data are expressed as means +/- SD relative to the control. Significance was determined by Student's t-test (two tailed, unpaired) * $p<0,05$, ** $p<0,01$.

5. DISCUSSION

Apoptosis of macrophages in the arterial wall is a hallmark in the development of atherosclerosis (27). Accumulation of apoptotic cells along with a transition to cell necrosis contribute to the destabilization of atherosclerotic plaques followed by plaque rupture and thrombus formation (28). The endpoint of the development of such a chronic disease may be myocardial infarction or stroke. From *in vitro* experiments it is known that the interaction of oxidized lipoproteins with cultured macrophages is responsible for the various facets of cell fate under pathophysiological conditions (23). oxLDL, characterized by a high content of modified lipid and protein components, is incorporated into the cells via scavenger receptors without a regulatory feedback mechanisms. As a consequence, lipids accumulate inside the cells and foam cells are formed. In mmLDL, a significant fraction of cholesterol and (phospho)lipid esters containing polyunsaturated fatty acids is modified or fragmented, but the apolipoprotein B (apoB) is hardly affected (29). These particles are also very toxic to macrophages and other cells of the vascular wall, depending on the extent of lipoprotein modification, dose and incubation time. mmLDL is still recognized by the apoB receptor, but its toxicity does not depend on receptor-mediated uptake of the entire particle (7). OxPL and especially those containing fragmented acyl chains are more polar and can be efficiently transferred to cell plasma membranes through the aqueous phase (Stemmer et al. submitted). Sustained exposure to mmLDL induces apoptosis in cultured vascular cells and macrophages (3,4,7), which is mediated by the activation of an aSMase generating the apoptotic lipid messenger ceramide. We have already shown that the truncated phospholipids PGPC and POVPC mimic the toxic effects of

mmLDL in cultured vascular smooth muscle cells (7). Here we provide evidence that both oxPL induce apoptosis in cultured macrophages. In these studies, we used RAW 264.7 macrophage-like cells and BMM. The tendencies of PGPC and POVPC to induce apoptosis were the same in both cell types, the bone marrow-derived cells being slightly more susceptible to oxPL toxicity than the RAW 264.7 cells. The mechanisms of oxPL toxicity in RAW 264.7 cells were studied in more detail and seem to differ from the pathways observed in cultured smooth muscle cells. POVPC rapidly activated aSMase in cultured RAW 264.7 macrophages. If activity of aSMase was inhibited by NB19, cells became more resistant to POVPC-induced apoptosis, showing that the activity of this enzyme is causally linked to POVPC toxicity in macrophages. Similarly, apoptosis induced by Jurkat cell-derived microparticles in RAW 264.7 macrophages was reduced when the cells were treated with an aSMase inhibitor (30). However, it has to be emphasized that the (oxidized) lipid composition of microparticles is complex and therefore it is not possible to attribute toxic effects to discrete molecular species. PGPC showed a small inhibitory effect on aSMase after 15 minutes incubation time. Data from preliminary experiments support the assumption that PGPC interferes with the enzymes of *de novo* ceramide synthesis localizing to intracellular membranes (endoplasmic reticulum), whereas aSMase is likely to generate ceramide in the plasma membrane (Koller, Marlingapla Halasiddappa, Hermetter, unpublished). The obviously different roles of ceramide-generating pathways in PGPC- and POVPC-induced macrophage apoptosis are due to the small structural differences in the short-chain carboxylic acids that are the remnants of arachidonic acid oxidation in position *sn*-2 of the parent glycerophospholipids. PGPC contains a carboxylic function at the ω-position of the truncated acyl chain, whereas POVPC contains a chemically reactive aldehyde group. PGPC can only physically interact with the biomolecules in its immediate

vicinity. It is rapidly internalized by the cells (31) and thus can influence the metabolic activities (ceramide synthesis) inside the cells. In contrast, POVPC is retained in the plasma membrane due to covalent Schiff base formation with the free amino groups of proteins and aminophospholipids (Stemmer et al, submitted). This behaviour is in line with the observation that POVPC rapidly activates aSMase which localizes at least in part to the cell surface.

In addition to diacylglycerophospholipids (mainly phosphatidylcholine), LDL also contains smaller amounts of alk(en)yl-acyl-analogs. Animal and human cell membranes, except the liver, may even contain large amounts of this phospholipid subclass (24,32-34). Most alk(en)ylacyl phospholipid species (mainly containing phosphocholine- and ethanolamine head groups) also contain polyunsaturated fatty acyl chains in position *sn*-2 of glycerol and therefore are subject to modification by reactive oxygen species (11). We found that the alkylacyl analogs of PGPC and POVPC are more potent inducers of apoptosis in RAW 264.7 macrophages than their diacyl counterparts. The same effects were also observed in cultured vascular smooth muscle cells (unpublished). Currently, we do not know the reason for the higher ether lipid toxicities, which may be due to differences in biochemical stability and biophysical properties in the cell (35). The *sn*-1 alkylether bond is resistant to hydrolytic cleavage and thus increases biochemical stability of the lipid molecule. From biophysical studies it is known that alkylacyl phospholipids are more densely packed (36) and increase the tendency of the membrane or some membrane areas to adopt nonbilayer lipid phases leading to membrane destabilization and alterations of membrane-associated enzyme functions.

One of the most striking phenomena of apoptosis is the controlled disintegration of cell (membrane) structures as a consequence of membrane blebbing, which is the

release of microparticles (apoptotic blebs) into the immediate environments or the circulation. These particles are enriched in oxPL (mainly PGPC, POVPC and PEIPC) (18,37) and thus must be considered vehicles of toxic compounds that trigger detrimental effects far from the site of their formation. As a consequence they can propagate apoptotic and inflammatory processes within the same tissues or other organs (38,39). The formation of microparticles may be favoured by the physical properties of the truncated phospholipids themselves (31) and/or the ceramide that is formed during the progress of apoptosis (40). We found that PGPC leads to massive microparticle formation whereas POVPC induced a much smaller vesicle release. The molecular shape of PGPC is conical and therefore it can directly induce high membrane curvature, a prerequisite for membrane vesiculation. The role of ceramide in PGPC-induced membrane blebbing is not obvious. PGPC seems to affect intracellular ceramide formation and to date it is unclear how the sphingolipid can reach the plasma membrane and contribute to cell surface-associated membrane effects under oxPL stress. A role of ceramide in POVPC-induced membrane blebbing is more plausible. The latter phospholipid stimulates aSMase and as a consequence ceramide can directly be generated in the plasma membrane. A direct contribution of POVPC to microparticle formation can not be inferred from the currently available information. The preparation of typical lipid-lipid and lipid-protein conjugates of POVPC, which forms Schiff bases with free amino groups of proteins and aminophospholipids, is under way in our laboratory in order to characterize the biophysical properties and cellular effects of these membrane-associated components.

In summary, PGPC, POVPC and their 1-O-alkyl analogs induce apoptosis in cultured macrophages, PGPC and ether- PGPC being more toxic than the POVPC counterparts. The higher toxicities of the former lipids are associated with more

severe consequences of the cells. Loss of plasma membrane vesicles is more efficient, if cells are exposed to PGPC. This result is physiologically highly relevant. Apoptotic blebs contain large amounts of oxPL and can carry these toxic compounds far away from site of production (18). Thus the biological activity of oxPL is potentiated by this process. Finally, the apoptotic effects of POVPC and its ether analog are coupled to the activity of aSMase. It remains to be elucidated, which pathway accounts for the formation of toxic ceramide under the influence of PGPC.

6. ABBREVIATIONS

aSMase: acid sphingomyelinase

BMM: bone marrow- derived macrophages

DMEM: Dulbecco's modified Eagle medium

E-PGPC: 1-O-hexadecyl-2-glutaroyl-*sn*-glycero-3-phosohcholine

E-POVPC: 1-O-hexadecyl-2-(5-oxovaleroyl)-*sn*-glycero-3-phosohcholine

EtOH: Ethanol

FACS: fluorescence activated cell sorting

FCS: Fetal calf serum

JNK: c-Jun N-terminal kinase

LDL: low-density lipoprotein

LPDS: lipoprotein deficient serum

MAPK: mitogen- activated protein kinase

MCSF: macrophages colony-stimulating factor

mmLDL: minimally modified low-density lipoprotein

MTT: 3-(4,5-dimethylthiazol-2-yl)-2,5-diphenyltetrazolium bromide

NBD: nitrobenzoxadiazole

oxLDL: oxidized low-density lipoprotein

oxPL: oxidized phospholipids

PAF: platelet activating factor

PEIPC: 1- palmitoyl-2-(5,6-epoxyisoprostane)-*sn*-glycero-3-phosphocholine

PGPC: 1- palmitoyl-2-glutaroyl-*sn*-glycero-3-phosphocholine

PLPC: 1- palmitoyl-*sn*-glycero-3-phosphocholine

POPC: 1- palmitoyl-2-oleoyl-*sn*-glycero-3-phosphocholine

POVPC: 1- palmitoyl-2-(5-oxovaleroyl)-*sn*-glycero-3-phosphocholine

TLC: thin-layer chromatography

7. ACKNOWLEDGEMENTS

This work was financially supported by the Austrian Science Fund FWF (project F30-B05 - special research program SFB *Lipotox*) and ESF EuroMEMBRANE CRP OXPL (project I308-B12).

8. REFERENCES

1. Watson, A. D., Leitinger, N., Navab, M., Faull, K. F., Horkko, S., Witztum, J. L., Palinski, W., Schwenke, D., Salomon, R. G., Sha, W., Subbanagounder, G., Fogelman, A. M., and Berliner, J. A. (1997) *J.Biol.Chem.* **272,** 13597-13607

2. Kolodgie, F. D., Narula, J., Burke, A. P., Haider, N., Farb, A., Hui-Liang, Y., Smialek, J., and Virmani, R. (2000) *Am.J.Pathol.* **157,** 1259-1268

3. Steinbrecher, U. P., Gomez-Munoz, A., and Duronio, V. (2004) *Curr.Opin.Lipidol.* **15,** 531-537

4. Deigner, H. P., Claus, R., Bonaterra, G. A., Gehrke, C., Bibak, N., Blaess, M., Cantz, M., Metz, J., and Kinscherf, R. (2001) *FASEB J.* **15,** 807-814

5. Seimon, T. A., Nadolski, M. J., Liao, X., Magallon, J., Nguyen, M., Feric, N. T., Koschinsky, M. L., Harkewicz, R., Witztum, J. L., Tsimikas, S., Golenbock, D., Moore, K. J., and Tabas, I. (2010) *Cell Metab* **12,** 467-482

6. Kinscherf, R., Claus, R., Deigner, H. P., Nauen, O., Gehrke, C., Hermetter, A., Russwurm, S., Daniel, V., Hack, V., and Metz, J. (1997) *FEBS Lett.* **405,** 55-59

7. Loidl, A., Sevcsik, E., Riesenhuber, G., Deigner, H. P., and Hermetter, A. (2003) *J.Biol.Chem.* **278,** 32921-32928

8. Ohanian, J., Liu, G., Ohanian, V., and Heagerty, A. M. (1998) *Acta Physiol Scand.* **164,** 533-548

9. Subbanagounder, G., Watson, A. D., and Berliner, J. A. (2000) *Free Radic.Biol.Med.* **28,** 1751-1761

10. Fruhwirth, G. O., Moumtzi, A., Loidl, A., Ingolic, E., and Hermetter, A. (2006) *Biochim.Biophys.Acta* **1761,** 1060-1069

11. Marathe, G. K., Davies, S. S., Harrison, K. A., Silva, A. R., Murphy, R. C., Castro-Faria-Neto, H., Prescott, S. M., Zimmerman, G. A., and McIntyre, T. M. (1999) *J.Biol.Chem.* **274,** 28395-28404

12. Deigner, H. P. and Hermetter, A. (2008) *Curr.Opin.Lipidol.* **19,** 289-294

13. Fruhwirth, G. O., Loidl, A., and Hermetter, A. (2007) *Biochim.Biophys.Acta* **1772,** 718-736

14. Friedman, P., Horkko, S., Steinberg, D., Witztum, J. L., and Dennis, E. A. (2002) *J.Biol.Chem.* **277,** 7010-7020

15. Moumtzi, A., Trenker, M., Flicker, K., Zenzmaier, E., Saf, R., and Hermetter, A. (2007) *J.Lipid Res.* **48,** 565-582

16. Hermetter, A., Stutz, H., Franzmair, R., and Paltauf, F. (1989) *Chemistry and Physics of Lipids* **50,** 57-62

17. Batzri, S. and Korn, E. D. (1973) *Biochim.Biophys.Acta* **298,** 1015-1019

18. Huber, J., Vales, A., Mitulovic, G., Blumer, M., Schmid, R., Witztum, J. L., Binder, B. R., and Leitinger, N. (2002) *Arterioscler.Thromb.Vasc.Biol.* **22,** 101-107

19. Bradford, M. M. (1976) *Anal.Biochem.* **72,** 248-254

20. Fling, S. P. and Gregerson, D. S. (1986) *Anal.Biochem.* **155,** 83-88

21. Vaskovsky, V. E. and Kostetsky, E. Y. (1968) *J.Lipid Res.* **9,** 396

22. Loidl, A., Claus, R., Deigner, H. P., and Hermetter, A. (2002) *J.Lipid Res.* **43,** 815-823

23. Glass, C. K. and Witztum, J. L. (2001) *Cell* **104,** 503-516

24. Schmid, H. H. and Takahashi, T. (1968) *Biochim.Biophys.Acta* **164,** 141-147

25. Aupeix, K., Hugel, B., Martin, T., Bischoff, P., Lill, H., Pasquali, J. L., and Freyssinet, J. M. (1997) *J.Clin.Invest* **99,** 1546-1554

26. Zhang, J., Reedy, M. C., Hannun, Y. A., and Obeid, L. M. (1999) *J.Cell Biol.* **145,** 99-108

27. Tabas, I., Williams, K. J., and Boren, J. (2007) *Circulation* **116,** 1832-1844

28. Tabas, I. (2004) *Cell Death.Differ.* **11 Suppl 1,** S12-S16

29. Salvayre, R., Auge, N., Benoist, H., and Negre-Salvayre, A. (2002) *Biochim.Biophys.Acta* **1585,** 213-221

30. Distler, J. H., Huber, L. C., Hueber, A. J., Reich, C. F., III, Gay, S., Distler, O., and Pisetsky, D. S. (2005) *Apoptosis.* **10,** 731-741

31. Rhode, S., Grurl, R., Brameshuber, M., Hermetter, A., and Schutz, G. J. (2009) *J.Biol.Chem.* **284,** 2258-2265

32. Heery, J. M., Kozak, M., Stafforini, D. M., Jones, D. A., Zimmerman, G. A., McIntyre, T. M., and Prescott, S. M. (1995) *J.Clin.Invest* **96,** 2322-2330

33. Marathe, G. K., Harrison, K. A., Murphy, R. C., Prescott, S. M., Zimmerman, G. A., and McIntyre, T. M. (2000) *Free Radic.Biol.Med.* **28,** 1762-1770

34. Tokumura, A., Toujima, M., Yoshioka, Y., and Fukuzawa, K. (1996) *Lipids* **31,** 1251-1258

35. Sommer, A., Paltauf, F., and Hermetter, A. (1990) *Biochemistry* **29,** 11134-11140

36. Smaby, J. M., Hermetter, A., Schmid, P. C., Paltauf, F., and Brockman, H. L. (1983) *Biochemistry* **22,** 5808-5813

37. Huber, L. C., Jungel, A., Distler, J. H., Moritz, F., Gay, R. E., Michel, B. A., Pisetsky, D. S., Gay, S., and Distler, O. (2007) *Apoptosis.* **12,** 363-374

38. Shih, P. T., Elices, M. J., Fang, Z. T., Ugarova, T. P., Strahl, D., Territo, M. C., Frank, J. S., Kovach, N. L., Cabanas, C., Berliner, J. A., and Vora, D. K. (1999) *J.Clin.Invest* **103,** 613-625

39. Yang, L., Latchoumycandane, C., McMullen, M. R., Pratt, B. T., Zhang, R., Papouchado, B. G., Nagy, L. E., Feldstein, A. E., and McIntyre, T. M. (2010) *J.Biol.Chem.* **285,** 22211-22220

40. Holopainen, J. M., Lehtonen, J. Y., and Kinnunen, P. K. (1997) *Chem.Phys.Lipids* **88,** 1-13

CHAPTER 3:

UPTAKE AND PROTEIN TARGETING OF FLUORESCENT OXIDIZED PHOSPHOLIPIDS IN CULTURED RAW 264.7 MACROPHAGES

U. Stemmer[1], E. Zenzmaier[1], B. Stojčić[1], G. Rechberger[2], M. Kollroser[3], and A. Hermetter[1]

[1] Institute of Biochemistry, Graz University of Technology, A-8010 Graz, Austria

[2] Institute of Molecular Bioscience, University of Graz, A-8010 Graz, Austria

[3] Institute of Forensic Medicine, Medical University of Graz, A-8010 Graz, Austria

1. ABSTRACT

The truncated phospholipids 1- palmitoyl-2-(5-oxovaleroyl)-*sn*-glycero-3-phosphocholine (POVPC) and 1- palmitoyl-2-glutaroyl-*sn*-glycero-3-phosphocholine (PGPC) are oxidation products of 1-palmitoyl- 2- arachidonoyl phosphatidylcholine. Both lipids are characterized by a short polar fatty acyl chain in position *sn*-2 and a hydrophobic, long fatty acyl chain in position *sn*-1 of glycerol. Depending on concentration and the extent of modification, these compounds induce growth and death, differentiation and inflammation of vascular cells thus playing a role in the development of atherosclerosis.

We found that sustained exposure to POVPC and PGPC induced apoptosis in cultured vascular cells, which is mediated by the second messenger ceramide. Here we describe the import of fluorescent POVPC and PGPC analogs into cultured RAW 264.7 macrophages and the identification of their primary protein targets. We found that the fluorescent oxidized phospholipids (oxPL) were rapidly taken up by the cells. The cellular target sites depended on the chemical reactivity of these compounds but not on the donor (aqueous lipid suspension, albumin or LDL). The great differences in cellular uptake of PGPC and POVPC are a direct consequence of the subtle structural differences between both molecules. The former compound (carboxyl lipid) can only physically interact with the molecules in its immediate vicinity. In contrast, the aldehydo- lipid covalently reacts with free amino groups of proteins and amino-phospholipids by forming covalent Schiff bases, and thus becomes trapped in the cell surface.

However, POVPC is freely exchangeable not only between donors and cell but also between the donors themselves, since imines are subject to protein- catalyzed base

exchange. Protein targeting by POVPC is a selective process since only a limited subfraction of the total proteome was labeled by the fluorescent aldehydo-phospholipid. Chemically stabilized lipid-protein conjugates were isolated from cultured macrophages and identified by MS/MS. The respective proteins are involved in apoptosis, stress response, lipid metabolism and transport. The identified target proteins may be considered as primary signaling platforms of the apoptotic oxidized phospholipid.

2. INTRODUCTION

The uptake of oxidized LDL (oxLDL) by the macrophages of the vascular wall is a hallmark of atherosclerosis (1). This process is mediated by the scavenger receptor and is not regulated. As a consequence, massive amounts of lipid accumulate in these cells. The macrophages change their phenotype and become foam cells, leading to the formation of fatty streaks in the subendothelial space, an early sign of the disease. The binding of oxLDL to the scavenger receptor is driven by an increase in net negative charge on the particle surface due to covalent modification of apoB lysines by lipid aldehydes that are oxidation products of polyunsaturated (phospho)lipids (2). To some extent, oxidized fatty acids and phospholipids containing free carboxyl groups also contribute to this characteristic signature of oxLDL. The harmful effects of oxLDL are not only associated with lipid accumulation in macrophages and other vascular (smooth muscle) cells (lipotoxicity). They are also mediated by the intrinsic toxicity of a great variety of lipid oxidation products that are generated in LDL under the conditions of oxidative stress (lipid toxicity) (3,4). These compounds comprise oxidized sterols, oxidized fatty acid derivatives and oxidized glycerolphospholipids. They have been found in plasma LDL and in lipid deposits as well as lipoproteins isolated from atherosclerotic plaques (5).

The main phospholipid species in the LDL surface contain linoleic and to a lesser extent arachidonic acid in position *sn*-2 of glycerol (6). Their oxidation products may contain a modified long-chain carboxylic acid in this position or a truncated acyl residue with a polar functional group at its ω-end. Typical derivatives of truncated phospholipids are the chemically reactive aldehydo-phospholipids POVPC and Poxno-PC (from arachidonoyl- and linoleoyl phospholipids, respectively) and the

carboxy-phospholipids PGPC and Paze-PC (also from arachidonoyl- and linoleoyl phospholipid, respectively).

We found that sustained exposure towards µM concentrations of both phospholipids classes induce apoptosis in vascular cells including vascular smooth muscle cells (7) and macrophages (Stemmer et al., unpublished data- see chapter 2). Programmed cell death is mediated by ceramide which is formed as a consequence of the rapid activation of acid sphingomyelinase (aSMase), very likely on the protein level (8). The same effects were observed, when the cells were treated with mmLDL under the same conditions. This particle can be obtained by mild oxidation of LDL *in vitro* and is perhaps a reliable model for the oxLDL formed *in vivo*. It is characterized by a high content of lipid oxidation products and a low degree of protein modification. Therefore, it is still recognized by the LDL receptor. As a consequence its toxicity must be largely due to the effects of its oxidized (phospho)lipid components.

Truncated phospholipids contain only a single hydrophobic long-chain fatty acid in position *sn*-1 attaching the amphiphile to the hydrophobic domain of the bilayer. From molecular dynamics studies, it can be inferred that the truncated *sn*-2 fatty acid folds back to the aqueous phase (carboxylic-phospholipids) or the lipid-water interface (aldehydo-phospholipids) (9). Therefore, these compounds show similar (supra)molecular features compared with other biologically active phospholipids, namely lysolecithin and platelet activating factor (PAF) (5).

Uptake and activity of oxidized phospholipids (oxPL) in cells has extensively been discussed in the context of receptor-mediated processes. Typical candidates are CD36 recognizing negatively charged motifs, e.g. due to carboxy-phospholipids, or the PAF receptor with affinities for choline phospholipids containing short *sn*-2 acyl chains (10). In addition to the capacity of the oxPL to interact with receptors, their

highly amphipathic character contributes to their cellular activities. Unlike entirely water-soluble receptor ligands, they efficiently partition into phospholipid bilayers where they can affect the functions of membrane-bound (signaling) proteins either by direct interactions or in an indirect way by modulating lipid dynamics and organization. Thus, it is more likely that oxPL encounter many primary targets representing primary signaling platforms either in the plasma membrane or after rapid internalization inside the cells.

In this study we characterized the import of fluorescent analogs of the oxPL, POVPC and PGPC, into cultured RAW 264.7 macrophages and identified their potential primary protein targets. The fluorescently labeled lipid analogs (11) were used as molecular tools to visualize these processes and detect the lipid binding polypeptides. We found that the fluorescent oxPL were rapidly taken up by the cells. Lipid import and localization depended on the chemical reactivity of these compounds (aldehydo versus carboxylate derivative). The lipid donor (aqueous lipid suspension, albumin, LDL) hardly showed any effect, pointing to the transfer of single molecules between the donor and acceptor surfaces. Targeting of cellular proteins is a selective process since only a subfraction of the total proteome was labeled. The respective lipid associated proteins may be considered as primary signaling platforms of oxPL.

3. EXPERMENTAL PROCEDURE

3.1 MATERIAL

Oxidized phospholipids (PGPC and POVPC) and their fluorescent analogues (BY - PGPE and BY -POVPE) were synthesized in our laboratory as previously described (11). Chemicals for gel electrophoresis were from BioRad Laboratories (Hercules, CA), unless otherwise noted. Organic solvents and all other chemicals were purchased from Carl Roth (Karlsruhe, Germany) or Sigma-Aldrich (Steinheim, Germany). Tissue culture materials were obtained from Sarstedt (Nürmbrecht, Germany) or Greiner (Kremsmünster, Austria). Dulbecco's modified Eagle medium and heat-inactivated fetal bovine serum were from Invitrogen (Leek, Netherlands), PBS and other cell culture supplements were obtained from PAA (Linz, Austria), unless otherwise indicated.

3.2 LDL ISOLATION AND MODIFICATION

Human LDL was isolated from pooled fresh plasma (a kind gift of Dr. Gholam Ali Khoschsorur, University Hospital, Graz) by density ultracentrifugation in OptiSeal tubes using a Beckman NVT65 Rotor (12). The LDL fraction was collected and transferred into sterile septum vials (TechneVials, Mallinckrodt, Germany) und stored at 4°C until use within 2 weeks of isolation. Lipoprotein concentration is expressed in terms of protein content, which was measured in a plate assay according to the method of Bradford (13). LDL was desalted using PD 10 columns (GE healthcare, Munich, Germany) prior to modification or labeling and diluted to 50 or 100 µg protein /ml, if not stated otherwise. Minimally modified LDL (mmLDL) was prepared as previously described (14). LDL was incubated with 10 µM $FeSO_4$ in sterile H_2O at

room temperature for 24 hours. mmLDL was desalted using PD 10 column (GE healthcare, Munich, Germany) prior to use.

3.3 DELIVERY SYSTEMS FOR FLUORESCENTLY LABELED oxPL

Lipid dispersions containing 5 or 10 µM lipid in PBS buffer were prepared using the ethanol injection method (15). The final ethanol concentrations did not exceed 1% (v/v). Albumin- oxPL complexes (protein/lipid = 1/1 mol/mol) were prepared, using the same technique. For this purpose, ethanolic solutions of oxPL were injected into solutions of BSA in PBS under stirring at 37 °C. Concentration of fluorescent oxPL was 5 µM. (mm)LDL-oxPL complexes (apoB100/oxPL= 20/1 mol/mol) were prepared by injection of ethanolic lipid solutions into LDL suspensions (50µg protein/ml) at 37°C followed by incubation at room temperature for 30 minutes. Total oxPL concentrations were 5 µM. Labeled LDL preparations were analyzed using native agarose gel electrophoreses (0,5% agarose gel, 80 V). Fluorescently labeled LDL was visualized in-gel using a Herolab imager (excitation wavelength: 365 nm) driven by EasyWin software. Total protein was stained with Comassie blue (0,02%, w/v). Fluorescently labeled proteins in albumin and LDL preparations were precipitated according to Wessels and Flügge (16), separated by SDS PAGE (4,5% Stacking gel, 10% resolving gel) according to Fling and Gregerson (17) and visualized using a BioRad laser scanner (Ex 488 nm, Em 530/30 BP). Finally, total protein was stained using Sypro Ruby ™ (Invitrogen) according to manufacturer's instruction. SDS gels were scanned for fluorescence at 605 nm upon excitation with a 488 nm laser. Incubations of the cells with pure lipid dispersions or lipid- carrier complexes were performed in PBS or media without phenol red at varying concentrations of FBS (0-10% v/v).

3.4 CELL CULTURE

The macrophage cell line RAW 264.7 (ATCC No. TIB-71, American Type Culture collection, Rockville, MD, USA) was a kind gift from Dagmar Kratky, Medical University of Graz, Austria. Cells were routinely grown in DMEM (4,5 g/l glucose, 25 mM HEPES, 4 mM L-Glutamine, without sodium pyruvate) supplemented with 10% heat- inactivated FBS and 100 U/ml penicillin/streptomycin at 37°C in humidified CO_2 (5%) atmosphere.

3.5 FLUORESCENCE MICROSCOPY

3.5.1 Uptake of BY-oxPL in RAW 264.7 macrophages.

Monolayer cultures of RAW 264.7 cells were grown to 60-80% confluence in Chamber slides (Nunc, Nalgene, Rochester USA). Cells were incubated with aqueous dispersions of oxPL or oxPL- carrier complexes (total concentrations of fluorescent oxPL were 5 or 10 µM) for 5 or 30 minutes, if not otherwise indicated. After incubation, cells were carefully rinsed with PBS and observed with an Axiovert 35 inverted fluorescence microscope equipped with a mercury-arc lamp and a CCD camera, driven by AxioVision software package (Carl Zeiss, Germany). BY-fluorescence (Ex 505 nm, Em 510 nm) was detected using the following filter set: Excitation filter BP 450-490 nm, Beam splitter 510 nm and barrier filter LP 520 nm. Unlabeled cells were used as a reference to examine autofluorescence.

3.5.2 Colocalization BY-oxPL with the plasma membrane

For fluorescence colocalization experiments monolayer cultures of RAW 264.7 cells were grown to 60-80% confluence in Chamber slides (Nunc, Nalgene, Rochester USA). Cells were incubated with 10 µM oxPL in PBS for 30 minutes. The labeled cells were rinsed twice with PBS prior to incubation with 5 µg/ml Cellmask Deep red plasma membrane stain diluted in PBS (Invitrogen) for 10 minutes. Finally, cells were

washed three times with PBS and BY fluorescence was observed with an Axiovert 35 inverted fluorescence microscope as described above. Cellmask fluorescence (Ex 649, Em 666) was detected using the following filter set: Excitation filter BP 575-625, Beam splitter 645 and Emission filter 660-710.

3.6 BY -POVPE EXCHANGE BETWEEN CELLS, LDL AND ALBUMIN

Solutions of BY -POVPE/LDL complexes in PBS (apoB /oxPL= 20/1 mol/mol, total oxPL concentration 5 µM) were desalted using PD 10 columns prior to incubation with 5 µM BSA solutions in PBS (molar ratios of apoB100/ albumin were 1:1, 1:5 and 1:10). The mixtures were incubated for 30 minutes at room temperature. Proteins were precipitated according to the method of Wessels and Flügge (16) and separated by SDS PAGE (17) (4,5% Stacking gel, 10% resolving gel). Fluorescently labeled proteins were detected using a BioRad laser scanner (Ex 488nm, Em 530/30). Backtransfer of BY -POVPE from cells to albumin was measured as follows: RAW 264.7 cells were grown to 60-80% confluence in 100 mm Petri dishes and treated with 6 ml of 5 µM fluorescent lipid in PBS as described above for 15 minutes. After washing the cells three times with PBS, 5 µM BSA in PBS was added followed by incubation at 37°C (5% CO_2) for 15 minutes. The supernatant was isolated and the fluorescent proteins were separated by SDS PAGE and imaged as described above.

3.7 DETERMINATION OF PROTEIN TARGETS OF BY-POVPE

3.7.1 Separation of total cell protein by 2-D electrophoresis:

RAW 264.7 cells grown to 80% confluence in 175 cm^2 culture flasks were incubated with 10 ml 10 µM BY -POVPE dispersion in PBS in the dark for 30 minutes. Labeled cells were washed twice with cold PBS and scraped into 3 ml washing solution (PBS supplemented with 100 mg/ml $CaCl_2$, 10 mg/ml $MgCl_2$, 1 mM PMSF and 50 µM $NaCNBH_3$). The following steps were performed at 4 °C. Cells were centrifuged at

300 g for 3 minutes. The supernatant was discarded, followed by cell lysis in 150 µl of lysis buffer, containing 20 mM HEPES, 2 mM EDTA, 1 % (v/v) Triton X-100 pH 7,4, 50 µM $NaCNBH_3$, 1 mM PMSF, 10 µg/ml SBTI, 10 µg/ml Leupeptin, for 1h on ice. The cell suspension was vigorously vortexed every 15 min. The lysate was centrifuged at 1000 g for 5 minutes. $NaCNBH_3$ was added to the supernatant (final concentration 100 µM). The resultant solution was incubated at 37°C for 2 hours and stored at -20 °C. Protein concentration was determined using a plate assay based on the method of Bradford (13). For 2-D PAGE on 20x20cm gels, 500 µg protein was precipitated by TCA or according to the method of Wessels and Flügge (16). The protein pellet was solubilized in 340 µl rehydration buffer, containing 7 M urea, 2 M thiourea, 4% Chaps, 0,002% bromphenol blue and 2% Pharmalyte ™ 3-10, at 37 °C for 30 minutes. Sample solutions were applied to 18 cm immobilized pH gradient strips pH 3-10 (GE healthcare, Munich, Germany). Strips were incubated over night at room temperature in the dark. Isoelectric focussing and subsequent SDS PAGE were performed as previously described (18). Electrophoretic separation of proteins was performed using a PROTEAN II Multi cell apparatus. After electrophoresis, gels were fixed in aqueous solution containing 10 vol. % EtOH, 7 vol. % AcOH, for at least 2 h. BY - fluorescence was detected using a BioRad laser scanner (Ex 488 nm, Em 530/30 BP). Total proteins were stained with Sypro Ruby™ (Ex 488nm, Em 605nm).

3.7.2 Separation of membrane proteins by 1-D gel electrophoresis

RAW 264.7 cells grown to 80% confluence in 175 cm^2 culture flasks were incubated with 10 ml aqueous solutions of BY -POVPE in the dark for 30 minutes. Labeled cells were washed twice with cold PBS and scraped into 10 ml PBS and isolated by centrifugation at 300 g for 5 minutes. The cell pellet was resuspended in 1 ml homogenization buffer (0,218 M Saccarose, 10 mM Tris/HCl, 1 mM EDTA, pH 7,4)

and separated by centrifugation at 450 g for 5 minutes. The pellet was resuspended in homogenization buffer (1,5 fold pellet volume) supplemented with Aprotinin, Pepstatin, Leupeptin, (10 µg/ml each), 0,8 mM PMSF, 30 µg/ml Cycloheximin and 50 µM $NaCNBH_3$. The following steps were performed at 4°C. Labeled cells were homogenized using a glass- glass homogenizer. The extent of homogenization was monitored by light microscopy. Homogenized cells were centrifuged at 600 g for 10 minutes. The post nuclear supernatant (PNS) was centrifuged again at 600 g for 5 minutes. The PNS was diluted with homogenization buffer containing the protease inhibitors indicated above (final volume 800 µl) and the sample was transferred into Beckmann centrifuge tubes (11x34) for ultracentrifugation (142000 g) at 4°C for 1 hour. The obtained supernatant represents the cytosolic fraction. The membrane pellet was washed in 800 µl homogenization buffer containing the protease inhibitors indicated above and centrifuged at 117000g at 4 °C for 1 hour. The membrane pellet was resuspended in 200 µl homogenization buffer. $NaCNBH_3$ (final concentration 100 µM) was added to the PNS, the cytosolic fraction and the membrane fraction followed by incubation at 37 °C for 2 h. Samples were stored at -20°C. For 1-D SDS PAGE, protein concentration was determined using a plate assay based on the method of Bradford (13). 100 µg protein of each sample were precipitated according to Wessel and Flügge (16) and dissolved in 50 µl loading buffer (17). The samples were applied onto a 20x20 cm SDS gel prepared and separated according to the PROTEAN II xi cell protocol provided by BioRad. Gels were fixed over night in aqueous solutions containing 10 vol. % EtOH, 7% vol. AcOH. BY- fluorescence was imaged using a Bio Rad Laser scanner (Ex 488 nm, Em 530/30 BP). Total proteins were stained with Sypro Ruby™ as indicated above.

3.7.3 Tryptic digest and MS/MS analysis

Fluorescent BY -POVPE- protein complexes were excised from acrylamid gels and tryptically digested according to the method of Shevchenko (19). Peptide extracts were dissolved in 0,1% formic acid and separated by nano-HPLC- system (ULTIMATE ™ 3000 nanoLC system, Dionex, Amsterdam, The Netherlands) as described (20), but using the following gradient: solvent A: water, 0,3% formic acid; solvent B: acetonitrile/water 80/20 (v/v), 0,3% formic acid; 0-5 min: 4% B, after 40 min 55% B, then for 5 min 90% B, and 47 min reequilibration at 4% B. The peptides were ionized in a Finnigan nano-ESI source equipped with Nanospray tips (PicoTip ™ Emitter; New Objective, Woburn, MA) and analysed in a Thermo-Finnigan LTQ linear iontrap mass-spectrometer (Thermo, San Jose, CA). The MS/MS data were analyzed by searching the National Center for Biotechnology Information nonredundant public database with SpektrumMill Rev.03.03.084 (Agilent, Darmstadt, Germany) software. Acceptance parameters were two or more identified distinct peptides according to Carr et al. (21). Identified protein sequences were subjected to BLAST and other public databases (Swiss-prot, Expasy, Brenda) to search for protein target candidates.

4. RESULTS

We report on the cellular uptake and the primary molecular targets of a subclass of oxidized phosphatidylcholines. The respective compounds contain a long-chain fatty acid in position *sn*-1 and a short, polar, acyl chain in position *sn*-2 of glycerol thus resembling the chemical structure of platelet activating factor (4,5). Specifically, we compared two compounds showing the same structural features except for the functional group at the ω-end of the *sn*-2 chain (Figure 1). In PGPC, this is a carboxylate residue which renders the entire molecule negatively charged. POVPC contains an aldehyde function which is less polar but chemically reactive and thus can undergo Schiff base formation with the free amino groups of proteins or phospholipids (22). In this study, we used BY- PGPE and BY- POVPE, as fluorescently labeled analogs of PGPC and POVPC respectively, carrying a polar BY-fluorophore linked to the polar lipid head groups (Figure 1) (11).

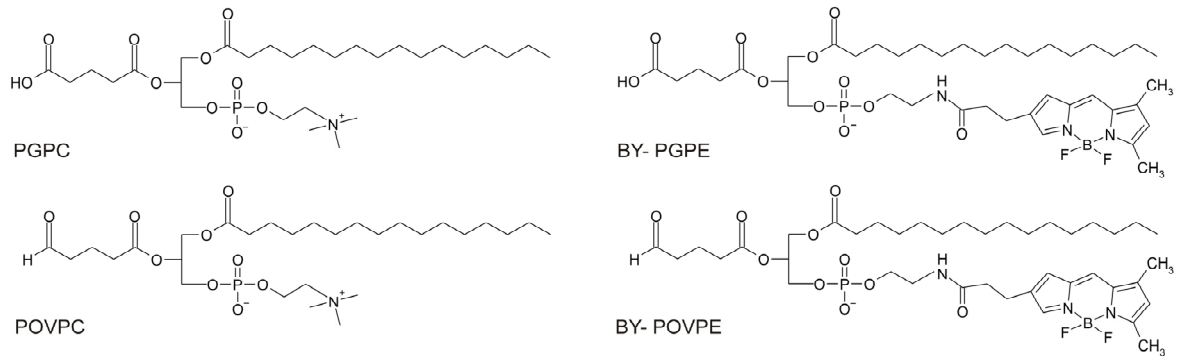

Figure 1: Chemical structures of oxPL and their fluorescent analogs

PGPC: 1-Palmitoyl-2-glutaroyl-*sn*-glycero-3-phosphocholine

BY- PGPE: 1-Palmitoyl-2-glutaroyl-*sn*-glycero-3-phospho-N- BODIPY™-ethanolamine

POVPC: 1-Palmitoyl-2-(5-oxovaleroyl)-*sn*-glycero-phosphocholine

BY- -POVPE: 1-Palmitoyl-2-(5-oxovaleroyl)-*sn*-glycero-phospho-N- BODIPY™-ethanolamine.

These compounds were used for visualization of lipids in live cells and lipid-protein complexes in acrylamide or agarose gels. In a previous study, we have provided evidence that they are reliable model compounds of their unlabeled counterparts (11).

Under physiological conditions, polar lipids can be transferred to cells from different molecular and supramolecular systems such as plasma proteins (albumin) and (low) density lipoproteins. Therefore, we prepared and characterized different donors containing the fluorescent lipid analogs and investigated the transfer of the labeled lipids from these systems to cultured macrophages using fluorescence microscopy. Conversely, we studied lipid transfer between the individual donors and the back-transfer of the lipids from the cells to the donors. Donor systems for our *in vitro* studies were defined complexes of the fluorescent lipids with albumin and LDL as well as aqueous lipid dispersions as reference systems. Figure 2 describes the characterization of BY- POVPE complexes with LDL and albumin. Agarose gel electrophoresis shows uniform bands of the fluorescent LDL (Figure 2 A). Fluorescence and protein detection demonstrate that the electrophoretic mobility of the labeled particle is higher as compared to unlabeled LDL. This effect is due to a more negative net charge which is a consequence of covalent modification of the LDL amino groups by the phospholipid aldehyde. SDS electrophoresis supports the assumption of an LDL-fluorophore complex containing covalently labeled apolipoprotein B (apo B) (Figure 2 B). No fluorescence is seen in apo B in SDS-PAGE after incubation with the carboxy lipid BY- PGPE because lipid-protein interaction is noncovalent in this system. The latter lipid can only be detected in LDL after running the labeled lipoprotein under conditions of native agarose gel electrophoresis (data not shown).

Both fluorescent oxPL form complexes with serum albumin. This observation is in line with the affinity of this protein for other phospholipids containing only one long-chain fatty acid (e.g. lysophospholipids) (23). BY- POVPE also forms a stable complex with albumin which is detectable by fluorescence imaging after SDS gel electrophoresis (Figure 2 B).

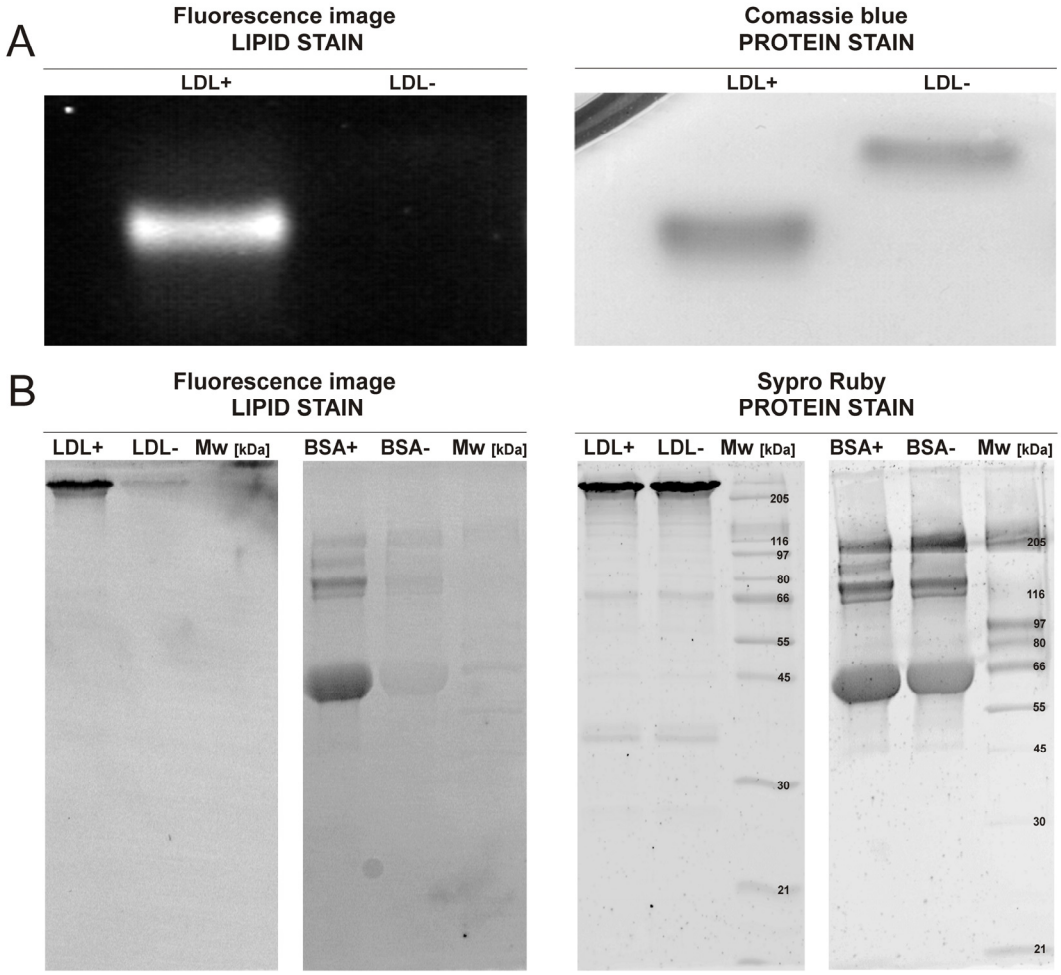

Figure 2 : Characterization of molecular and supramolecular carriers of BY- POVPE

(+ represents complexes labeled with BY- POVPE; - represents unlabeled references)

Panel A. Agarose gel electrophoresis (0,5%) of labeled LDL. LDL/ BY- POVPE complexes (20 / 1, mol / mol; 5 µM label) show uniform bands with higher mobility of the labeled particle which is due to a more negative net charge as a consequence of covalent modification of amino groups by the aldehydo lipid.

Panel B. SDS Page of labeled LDL and BSA: LDL/ BY- POVPE complexes (20 / 1, mol / mol; 5 µM label) and BSA/ BY- POVPE complexes (1 / 1, mol / mol; 5 µM label) show stable

labeling of LDL protein and BSA by the aldehydo lipid. Fluorescent images were obtained using a Herolab imager (Pane A) or a BioRad laser scanner (Panel B). PGPC interacts with its targets in a noncovalent manner. Therefore, it is not possible to visualize protein- BY-PGPE complexes on SDS gels. Only labeled LDL can be seen on agarose gels (data not shown).

In order to observe phospholipid transfer independent of receptor- mediated endocytosis, uptake of fluorescent oxPL into the cells was studied under growth conditions, where the LDL receptor was not expressed. BY- PGPE and BY- POVPE are taken up into these cells in a very different manner (Figure 3 A). BY- PGPE is quickly internalized. The amount of fluorophore residing in the plasma membrane must be negligible since only a small fraction of the fluorescent cellular lipid can be extracted by aqueous Triton X-100 (data not shown). The mechanism of lipid uptake has already been described in a previous publication. It has been shown that the fluorescent compound inserts into the plasma membrane followed by cluster formation within milliseconds(24). Eventually, the fluorescent domains are internalized by endocytosis.

The fluorescence intensity inside the cells was significantly lower if labeled LDL was the lipid donor. This lipoprotein contains PAF-acetylhydrolases which also catalyzes the degradation of short-chain oxPL leading to polar degradation products partitioning more efficiently into the aqueous phase (25). BY- POVPE almost entirely localizes to the cell surface (colocalization with a plasma membrane-specific dye; Figure 3 B), due to Schiff base formation with membrane proteins and amino phospholipids.

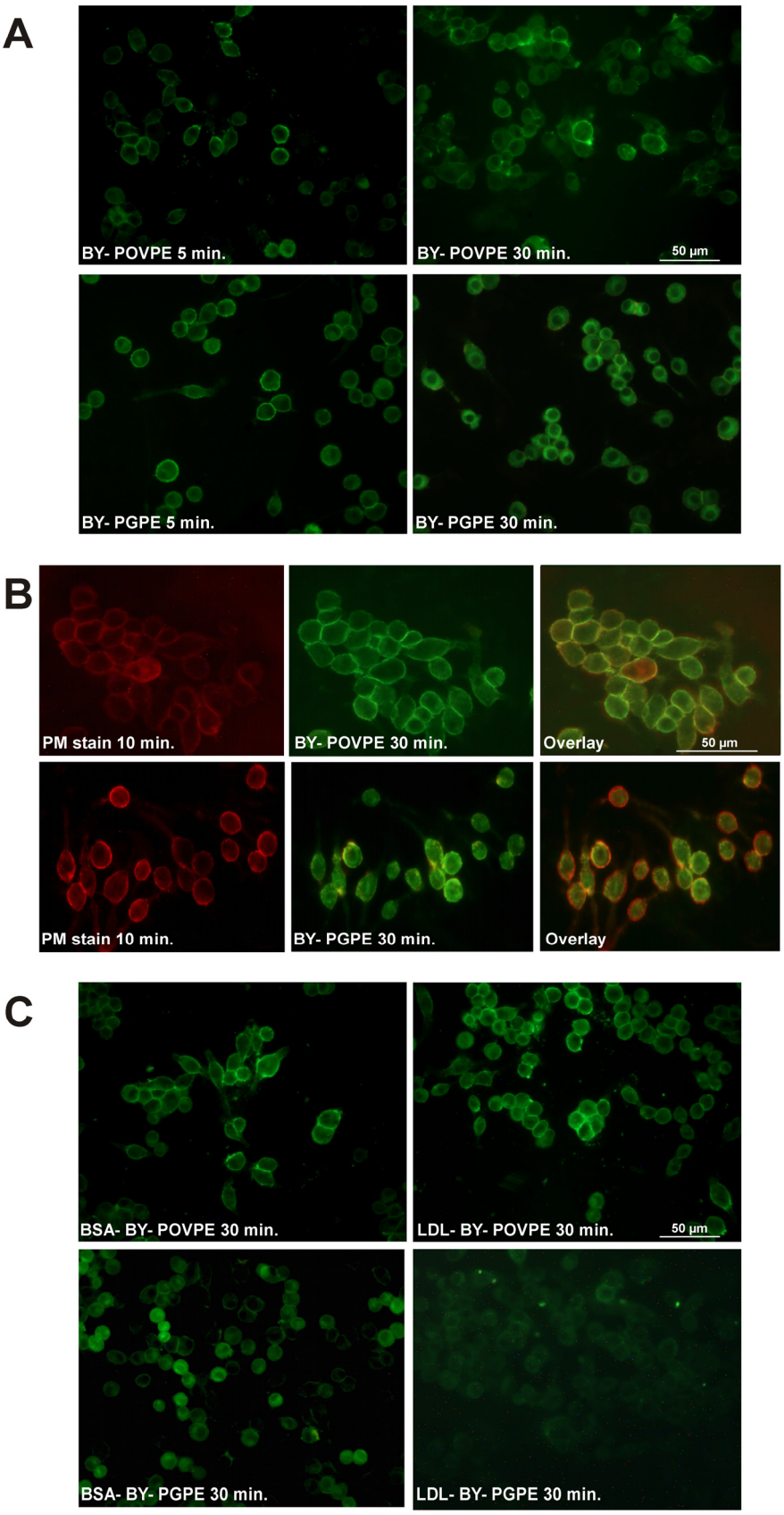

Figure 3: Uptake of oxPL by RAW 264.7 macrophages from different carriers

Panel A: Fluorescence micrographs (320x) of RAW 264.7 cells incubated with oxPL (5µM) suspensions in PBS over 5 and 30 minutes. BY- oxPL fluorescence is detected in the plasma membrane after 5 minutes incubation time. BY- PGPE is rapidly internalized by the cells. In contrast, BY-POVPE stays much longer in the plasma membrane due to formation of covalent adducts with free amino groups of proteins and lipids. Washing of labeled cells with 0,1% Triton-X-100 in PBS for 5 seconds removed a significant fraction oxPL from the plasma membrane, but only a small amount of lipid from the cell interior (data not shown).

Panel B: Image section of fluorescence micrographs (320x) of RAW 264.7 macrophages incubated with fluorescent oxPL (10 µM, suspension in PBS). After incubation cells were stained with Cell mask Deep red plasma membrane (PM) stain (5 µg/ml in PBS) for 10 minutes. BY- POVPE, but not BY- PGPE colocalized with the plasma membrane stain.

Panel C: Fluorescent micrographs (320x) of RAW 264.7 cells pre-incubated with BY- oxPL labeled BSA or LDL for 30 minutes. Similar patterns are found for oxPL uptake from different carriers (mmLDL showed similar patterns as LDL- data not shown). In case of BY- POVPE most of the fluorescence is detected in the plasma membrane where the fluorescent POVPC analog is captured by proteins and lipids. Only low amounts of the fluorescent PGPC analog is taken up by the cells from LDL or mmLDL. These low apparent uptake efficiencies are due to prior oxPL degradation in the lipoprotein. No autofluorescence was detected in unlabeled control cells (data not shown).

The lipid- protein complexes were stabilized by chemical reduction and identified as putative primary targets of the phospholipid aldehyde (see below). In summary, lipid uptake does not depend on the donor system. The same cellular fluorescence patterns were obtained if phospholipids were released to the cells from pure lipid dispersions, lipid-albumin complexes or lipid- loaded LDL (Figure 3 C).

Despite the fact that the lipid aldehyde BY- POVPE is firmly bound to LDL and albumin, it is released from these carriers to the phospholipids and proteins of the cell plasma membrane suggesting high reversibility of Schiff base formation. This observation prompted us to study the transfer of the aldehydo-phospholipid between the individual donor systems LDL and albumin on the one hand and the release of cellular phospholipid to albumin on the other hand.

Figure 4 A shows that BY- POVPE can be transferred from labeled LDL to unlabeled albumin in a concentration-dependent manner. After incubation of both “donor” systems followed by SDS electrophoresis, the fluorescence can be seen both in the apoB and the albumin band. The emission intensity correlated with the amount of albumin in the incubation mixture. Release of BY- POVPE from LDL is significantly reduced after treatment with $NaCNBH_3$ leading to the formation of stable amine bonds (data not shown). If cells labeled with BY- POVPE were incubated with unlabeled albumin, the same phenomenon was observed (Figure 4 B). The lipid fluorescence was detectable in the albumin band after SDS gel electrophoresis. The partitioning of the aldehydo-phospholipid between the different biological surfaces can be explained by the pK values of aliphatic Schiff bases around pK 7 (26). Under these conditions, a significant fraction of the imines in the protein and lipid complexes of BY- POVPE is protonated and therefore prone to nucleophilic attack by other amines in the sample.

We isolated and identified the protein targets of BY- POVPE in cultured macrophages, which are expected to form covalent Schiff base adducts (Figure 5). Because the imine complexes are unstable, they have to be stabilized before isolation and separation by chemical reduction leading to the formation of the stable amines.

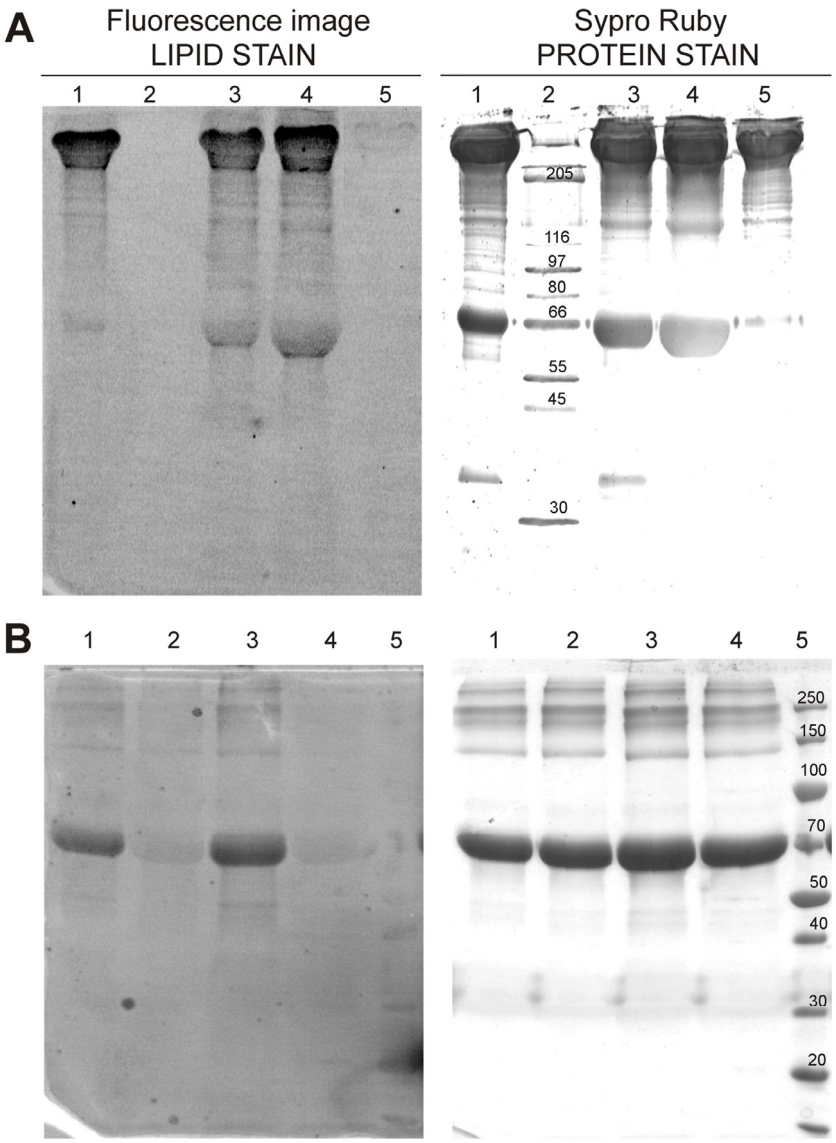

Figure 4: Transfer of BY- POVPE between lipid donors- Reversibility of Schiff base formation in BY- POVPE - protein complexes.

Panel A: LDL/ BY- POVPE complexes were incubated with various amounts of BSA followed by protein separation using SDS PAGE. Fluorescence imaging of labeled lipid- protein complexes on SDS gels shows that BY- POVPE is transferred from LDL to bovine serum albumin in a concentration-dependent manner, indicating that Schiff base formation between BY- POVPE and its targets is reversible. LDL has a higher capacity than BSA for accommodating BY- POVPE (apoB and phospholipids monolayer). If LDL- BY- POVPE complexes were stabilized by reduction of the Schiff bases prior to incubation with BSA, much lower fluorescent intensities were observed, indicating reduced exchangeability (data not shown). BY- POVPE exchange between the following systems was studied (mol LDL refers to the molar amounts of apoB100). Lane 1: LDL- BY- POVPE: BSA 1:1 mol/mol; Lane

2: MW Standard; Lane 3: LDL- BY- POVPE: BSA 1:5 mol/mol; Lane 4: LDL- BY- POVPE: BSA 1:10 mol/mol; Lane 5: LDL reference.

Panel B: RAW 264.7 cells were incubated with BY- POVPE (10µM) or without label (blank sample) for 15 min followed by extensive washing with PBS and adding of 10 µM BSA solution. This mixture was incubated for 15 minutes. The BSA containing supernatant of BY-POVPE treated (lanes 1 and 3) or blank samples (lanes 2 and 4) was collected and split into two aliquots. One sample was incubated under reducing conditions for 30 minutes to stabilize the Schiff base. The proteins were precipitated and separated by SDS gel electrophoresis prior to detection of fluorescence by Laser scanning and protein staining with Comassie blue. Without reductive stabilization of the Schiff base the same results were obtained, but the fluorescence intensities were much weaker. Lanes 1 and 2: 20µg Protein; Lanes 3 and 4: 40 µg Protein; Lane 5: MW Standard. Lanes 1 and 3 show that BY- POVPE is back-transferred from the cell surface to BSA. Fluorescence intensities depend on lipid acceptor concentration. The slight autofluorescence of BSA in Lanes 2 and 4 is due to the emission of bound Bilirubin.

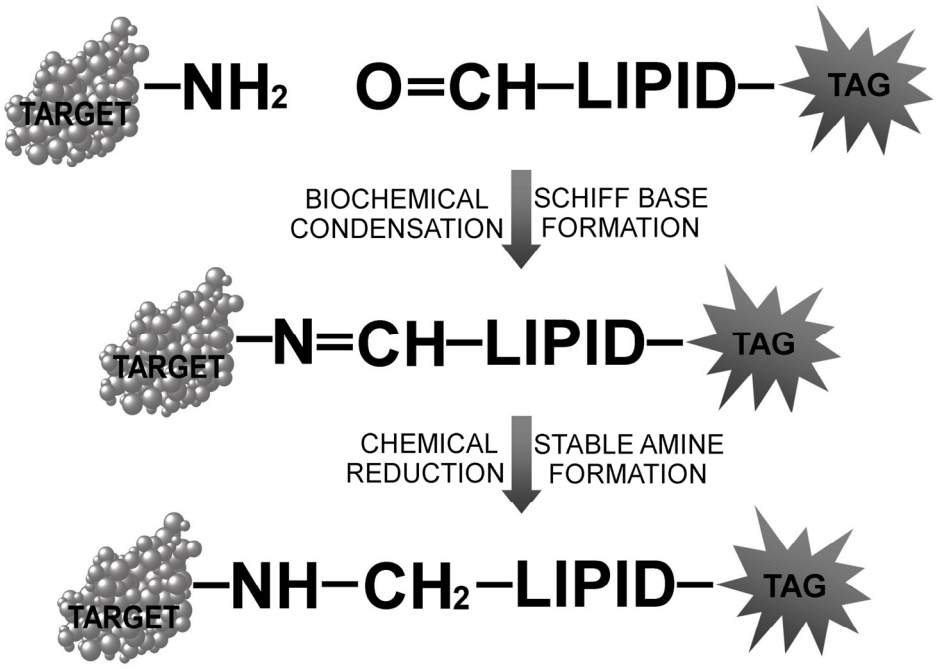

Figure 5: Covalent interaction of POVPC with protein and lipid targets

The aldehyde group at the truncated *sn*-2 chain of POVPC forms a covalent Schiff base with free amino groups of proteins and presumably aminophospholipids (PE and PS). Since Schiff bases are unstable, the imines are chemically reduced to the stable amines for further analysis

We used a proteome approach to identify the lipid binding proteins in total cell lysates as well as in the total membrane fractions. For this purpose, the cells were incubated with the fluorescent lipid, followed by lysis and isolation of total membranes by centrifugation. Proteins of total cell lysates were separated by 2-D PAGE (Figure 6 A), whereas the total membrane fraction was subjected to 1-D SDS electrophoresis (Figure 6 B). The fluorescent protein spots/ bands were excised and tryptically digested followed by MS/ MS analysis of the peptides. Figures 6 A and B show that the fluorescence patterns reflecting the labeled protein targets are much less complex than the total protein patterns detected after Sypro Ruby staining. Obviously, the protein targeting by the oxidized phospholipids is selective rather than random. This effect may be due to the different pK values of differently exposed amino groups and steric constrains as a consequence of different lipid-protein and protein-protein interactions in the membrane. The specific protein targeting by BY-POVPE is underscored by the data shown in Figure 6 B. The fluorescence image shows the protein targets of the phospholipid aldehyde in membranes depending on fluorophore concentration in the incubation medium. Higher lipid concentrations lead to uniformly higher fluorescence intensities of the individual bands, but the fluorescence pattern is always the same.

Obviously, protein modification by BY- POVPE is a selective process. According to the data in Tables 1 and 2, it affects polypeptides involved in membrane transport (e.g. VDAC), stress response (e.g heat shock proteins), apoptosis (e.g. CathepsinD, caspases) and lipid metabolism (e.g. N-acyl-sphingosine hydrolase) (Tables 1 and 2). In the membrane fraction and especially in the total cell lysate, we do not only find membrane but also cytosolic proteins. These targets may be labeled by a small fraction of lipid entering the cell interior. Once a cytosolic protein is alkylated by the

aldehydo-phospholipid, it becomes associated with lipid bilayers and, as a consequence, shows up in the membrane pellet after ultracentrifugation.

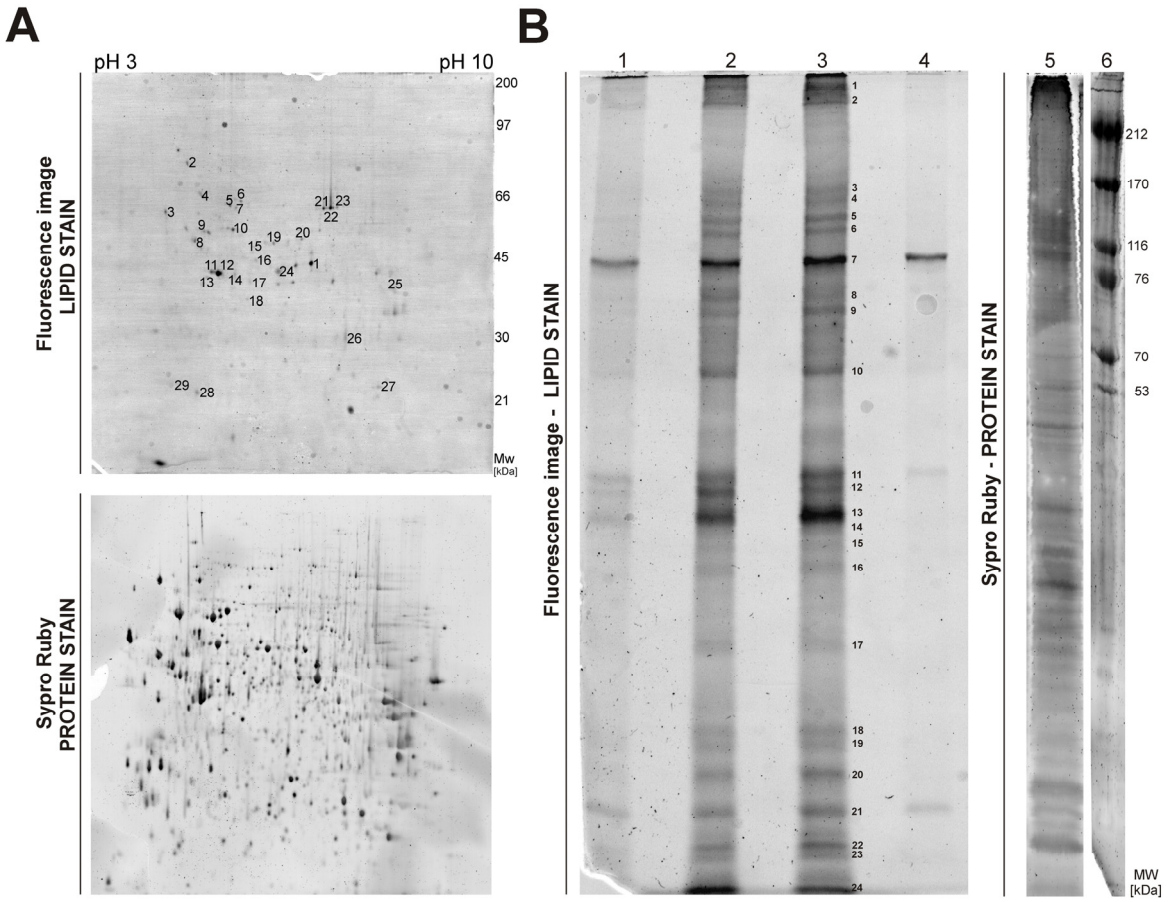

Figure 6: Protein targets of fluorescent BY- POVPE in RAW 264.7 macrophages

Panel A: Cells were incubated with BY- POVPE (10 µM) in PBS for 30 minutes followed by lysis under reductive conditions to stabilize the lipid-protein complexes (Schiff bases). The labeled proteins were precipitated and separated by 2-D SDS gel electrophoresis. Fluorescent proteins were imaged using a fluorescence laser scanner (Biorad). The lipid stain represents the proteins covalently attached to the fluorescent oxPL. The Sypro Ruby™ stain represents the full cell proteome. The fluorescence patterns show that the staining of the protein targets by BY- POVPE is a selective process affecting only a defined subset of the cell proteome.

Panel B: Cells were incubated with different concentrations of BY- POVPE in PBS over 30 minutes followed by separation of the membrane fraction using ultracentrifugation (> 100000 g). The membrane pellets were isolated and resuspended in PBS prior to protein

precipitation and separation by 1-D SDS gel electrophoresis. After incubation of the cells with the oxPL, all procedures were performed under reductive conditions (see above). Fluorescent proteins were imaged using a fluorescence laser scanner (Biorad). The lipid stain represents the proteins covalently attached to the fluorescent oxPL. BY- POVPE concentrations in the incubation mixtures: Lane 1: 1 µM; Lane 2: 2,5 µM ; Lane 3: 5 µM; Lane 4: 0 µM, shows only autofluorescent proteins; Lane 5: Sypro Ruby™ full protein stain of one representative lane, Lane 6: MW Standard. Fluorescence intensities of the BY- POVPE-labeled protein targets depend on lipid concentration and leveled off at 5 µM lipid. The fluorescent patterns and therefore the selectivity of labeling were unaffected by the amount of BY- POVPE.

Table 1: Protein targets of BY- POVPE in total RAW 264.7 macrophage lysates.

Grey bars indicate proteins also found in the membrane fractions (Table 2). Cells were incubated with BY- POVPE (10 µM) in PBS for 30 minutes followed by lysis and 2-D SDS gel electrophoresis. Spots (Figure 6 Panel A) were excised and tryptically digested. Subsequently, peptides were analyzed by MS/MS and targets were identified by data base search (NCBI, Expasy, Swiss-prot, Brenda).

Spot (#)	Spectra (#)	Distinct Peptides (#)	Distinct Summed MS/MS Search Score	AA Coverage [%]	Protein MW [Da]	Protein pI	Database Accession GI (#)	Proteinname
1	8	5	49,09	11	46798,50	5,97	26347479	sorting nexin 5
1	12	4	44,93	11	45771,10	6,23	148709540	leupaxin
2	154	25	384,54	35	92490,30	4,74	14714615	Heat shock protein 90kDA beta (Grp94)
3	8	4	53,45	10	48021,80	4,34	74227675	calreticulin
4	467	32	550,23	53	72422,40	5,07	2506545	78kDa glucose reulated protein precursur
5	173	20	336,08	36	70947,50	5,37	74198978	Dank-type molecular chaperone hsp72-ps1
5	37	10	158,11	19	72416,70	5,83	74192747	arginyl aminopeptidase
6	255	14	246,43	26	73528,70	5,91	6754256	heat shock protein 9 grp 75 Hsp709A
7	371	24	400,41	44	70947,50	5,37	74198978	Dank-type molecular chaperone hsp72-ps1
7	34	7	122,94	14	68368,50	5,42	31560731	ATPase, H+ transporting, lysosomal V1 subunit A
8	9	3	48,82	11	39370,90	4,95	148686207	lymphocyte specific 1
9	14	8	134,39	16	72477,50	5,10	2598562	BiP Hsp70 protein GRP78
9	6	3	40,65	6	57079,20	5,88	149023098	protein disulfid isomerase associated 3
10	70	14	190,29	31	56775,30	5,89	148691054	ubiquitin- specific peptidase 14
10	65	13	185,40	27	61054,90	6,07	51766670	heat shock protein 1 (chaperonin)
10	14	4	46,81	6	58928,90	5,48	74214557	copine I
11	202	7	120,29	21	45002,10	5,42	148673963	mCG13192 p47 protein
12	11	5	66,67	16	38358,20	5,17	6754910	mCG19035, nudC nuclear distribution gene C
12	3	2	22,20	4	53711,20	5,12	74184979	ataxin10
13	7	5	64,87	19	37402,30	5,06	7305121	glycogenin
14	21	7	111,06	21	38358,20	5,17	6754910	mCG19035, nudC nuclear distribution gene C
15	10	3	46,74	8	45565,50	5,86	74212703	RasGAP-associated protein p56dok-2
16	67	13	202,10	31	51146,80	5,49	70794778	RuvB-like 2
16	22	4	64,72	12	48374,20	6,85	26354406	cathepsinD
17	12	4	53,33	12	393514,00	5,44	27370510	paraoxonase3
17	5	2	35,39	6	37719,60	5,61	148683063	guanine nucleotide binding protein
18	3	3	33,73	10	35930,00	5,43	33416530	Annexin A4
19	27	11	139,71	26	51777,80	5,58	18017596	sorting nexin 4
19	50	10	133,75	20	57538,20	5,57	74191447	vacuolar H+ATPase B2
20	43	9	120,41	19	56585,90	8,30	5235955	3-phosphoglycerate dehydrogenase
21	13	5	66,45	9	72613,90	7,06	74219241	succinate dehydrognease Fp subunit
22	59	6	75,52	11	60630,40	6,28	6753320	chaperonin subunit 3
22	123	4	56,40	7	72613,90	7,06	74219241	succinate dehydrognease Fp subunit
23	75	12	203,43	24	75801,50	8,30	148704343	phosphoenolpyruvate carboxykinase 2
23	8	4	52,80	7	72613,90	7,06	74219241	succinate dehydrognease Fp subunit
24	4	2	26,11	5	46762,20	5,86	148704797	sorting nexin 6
24	11	6	83,96	15	45640,70	5,73	86198305	caspase1
25	3	2	25,95	5	44669,80	8,86	9790019	N-acyl shingosine amidohydrolase
26	22	6	88,00	22	31746,00	7,44	33243895	voltage dependent anion channel2 VDAC-2
26	10	3	41,70	16	31475,00	6,46	6753284	caspase3
27	8	3	42,05	16	22236,70	8,26	12846314	peroxiredoxin1
28	5	2	29,80	6	36856,50	4,72	7106546	LOC298795 protein, similar 14-3-3 sigma
29	14	4	65,88	15	29965,70	8,25	74185553	Tat-interacting protein TIP30
29	3	2	30,52	7	32577,80	7,67	74212025	voltage dependent anion channel VDAC-1

Table 2: Protein targets of BY- POVPE in the total membrane fraction of RAW 264.7 macrophages.

Grey bars indicate membrane-associated proteins. Cells were incubated with BY- POVPE (5 µM) in PBS for 30 minutes followed by the isolation of the total membrane fraction and 1-D SDS gel electrophoresis of the proteins. Bands (Figure 6 Panel B) were excised and

tryptically digested. Subsequently, peptides were analyzed by MS/MS and targets were identified by data base search (NCBI, Expasy, Swiss-prot, Brenda).

Band (#)	Spectra (#)	Distinct Peptides (#)	Distinct Summed MS/MS Search Score	AA Coverage [%]	Protein MW [Da]	Protein pI	Database Accession GI (#)	Proteinname
1	68	20	328,08	5	534218,4	5,74	122065897	Plectin-1
1	56	18	293,94	4	532048,3	6,03	134288917	dynein, cytoplasmic, heavy chain-1
2	138	21	357,47	10	272134,3	5,92	49022858	talin 1, isoform CRA_b
2	25	5	81,7	2	274938,7	6,16	148702862	fatty acid synthase, isoform CRA_b
2	3	2	25,43	1	125954,4	6,92	148704174	ATPase, aminophospholipidtransporter-like, class I
3	47	10	149,35	14	92771,4	4,72	14714615	rCG49111- Hsp90kDa beta (Grp94), member1
3	49	7	107,49	9	113054,9	5,30	6978543	ATPase, Na+/K+ transporter, alpha1 polypeptide
3	30	15	253,46	17	123093,4	5,72	38604071	exportin
3	14	3	55,49	4	91048,2	5,26	148670554	vasolin
3	3	2	36,05	4	85026,4	7,02	3183523	Integrin beta 2 precursor
4	33	7	114,46	11	84816,3	4,93	74147335	heat shock protein 1, alpha
4	29	12	203,06	21	67278,3	4,50	6671664	calnexin
5	140	28	482,63	45	83341,8	4,97	51859516	Hsp90
5	22	11	184,59	17	86295,4	7,02	148666539	inner mebrane protein
5	19	7	97,68	15	53748	5,06	74199770	vimentin
6	28	9	142,87	12	86295,4	7,02	148666539	inner membrane protein , mitochondrial
7	80	25	440,32	39	74300	6,54	12835914	Lamin A isoform A
7	39	16	277,7	28	70208,7	5,12	74139671	lymphocyte cytosolic protein 1
7	36	15	248,36	31	74570	8,43	27369581	solute carrier family 25
7	51	14	240,71	25	72613,9	7,06	74219241	succinate dehydrogenase Fp subunit
7	13	6	94,56	11	70947,5	5,38	74198978	Dank-type molecular chaperone hsp72-ps1
7	9	4	59,81	7	68528,7	6,02	48474583	Dolichyl-diphosphooligosaccaride-protein GT
7	7	2	32,39	4	71376,8	7,92	56550045	spleen tyrosin kinase
7	3	3	36,85	4	70208,7	5,12	7413967	65-kDa macrophage protein
7	2	2	26,97	3	69311,5	5,73	50510565	SWA-70 protein
8	262	28	500,67	62	57846,2	6,66	74221210	pyruvate kinase
8	29	11	199,54	27	59684,6	7,95	74151643	T-complex protein 1 subunit
8	22	14	218,65	28	58104,7	6,46	74204595	chaperonin subunit 6a
8	19	9	125,33	18	53748	5,06	74199770	vimentin
8	18	5	80,47	9	58084,7	8,24	74204209	chaperonin subunit 4 (delta)
8	13	8	123,87	19	56678,7	5,88	112293264	protein disulfid isomerase associated 3
8	6	2	30,56	4	57079,2	5,88	149023098	protein disulfid isomerase associated 3
8	5	3	41,14	8	57987,6	5,37	31543458	p21- activated kinase 2
9	165	18	343,58	49	56667,1	5,24	23272966	Atp5b protein
9	302	32	563,07	65	53687,9	5,06	31982755	vimentin
9	76	17	312,48	50	53811,8	8,10	148698452	CAP, adenylat cyclase-associated protein 1
9	72	17	244,43	36	53688,9	5,04	74139645	vimentin
9	62	19	345,6	53	57477,6	5,97	126521835	chaperonin subunit 2
9	53	17	300,52	38	59766,9	9,22	74211072	ATP synthase, H+ transporting
9	22	10	186,6	27	57538,2	5,58	74191447	vacuolar H+ ATPase B2
9	12	5	74,71	8	65442,5	9,27	50510859	sphingosine phosphate lyase
9	3	2	27,37	5	54305,1	8,28	16758554	phosphadidylinositol 4-kianse type2 alpha
10	18	5	74,8	12	51737	8,72	13385942	citrate synthase
10	10	3	54,98	11	48374,2	6,86	26354406	cathepsin D
11	232	5	82,95	18	33312,5	9,83	61556754	prohibitin 2
11	101	4	72,92	17	31746	7,44	13786202	voltage dependent anion channel 2
12	84	5	87,14	22	32351,6	8,55	10720404	voltage dependent anion channel 1
12	33	5	85,21	18	35148	7,60	74207645	guanine nucleotide binding protein
13	86	8	122,73	26	32931,5	9,74	22094075	solute carrier family 25, member 5
13	27	9	149,32	31	35096,8	5,36	74215924	14-3-3 gamma
13	12	6	118,01	33	29087,8	4,71	148676868	14-3-3 zeta
13	9	5	85,39	25	30884,1	8,96	5980769	voltage dependent anion chanel 3
13	8	2	38,55	11	25067,2	6,10	123234567	tumor protein D52-like 2
14	15	3	38,22	8	31611,1	9,20	148697937	B-cell receptor- associated protein 31
15	30	3	57,65	11	32191,9	5,57	148667347	Triphosphatisomerase
15	30	2	39,68	10	26927,2	4,92	70608194	tumor protein D52-like 2
16	22	2	41,4	12	31440,6	6,54	975689	stomatin
16	20	3	45,81	13	23927,1	5,85	16758368	RAB 14, member Ras oncogen family
17	15	5	92	25	22541,1	8,58	7710086	RAB 10, member Ras oncogen family
17	7	2	25,36	7	28144,9	9,55	148687100	RAS-related C3 botulinum substrate 1
18	320	4	54,53	16	20246,8	11,39	30061401	histone cluster 2, H3c1 isoform 2
18	42	3	53,13	28	11651	4,42	83745120	ribosomal protein, large P2
19	461	6	96,76	40	16572,4	10,13	149029297	histone 1, H2bn
19	127	3	59,3	30	14759	9,21	6677775	ribosomal protein L22
20	54	2	38,49	15	17748,7	10,85	149263957	ribosomal protein S18
21	152	5	90,57	32	17239,2	10,59	94378251	similar to histone 4
22	11	2	32,61	21	9326,8	9,52	33563266	NADH dehydrogenase 1 alpha subcomplex
23	58	2	35,12	21	9326,8	9,52	33563266	NADH dehydrogenase 1 alpha subcomplex
24	8	3	44,93	5	56505,3	5,10	57012436	keratin 10

5. DISCUSSION

Sustained exposure of cultured vascular cells to the truncated oxPL PGPC and POVPC leads to apoptotic cell death. A couple of receptors have so far been discussed as primary signaling platforms propagating the toxic lipid effects. Since both compounds are structurally related to platelet activating factor (PAF), they show binding affinities for the PAF receptor (27). Other receptor candidates have also been suggested including TLR-2 and CD 36 (28). The latter protein preferably binds lipid or protein domains with net negative charges and therefore is a receptor candidate for PGPC. This assumption is underlined by the Whisker model suggested by Greenberg et al (29). According to this hypothesis, oxPL mainly influence the properties of membrane surfaces via their polar acyl chains which protrude into the aqueous phase. This assumption has meanwhile been supported by molecular dynamic studies by Khandelia and Mouritsen on Paze-PC and Poxno-PC that are longer chain homologs of PGPC and POVPC, respectively (9).

Although many cellular effects of oxPL are mediated by receptors, it is unlikely that specific receptor binding is the only primary event responsible for lipid activity. In contrast to water-soluble peptides or small molecules as receptor ligands, (oxidized) phospholipids are amphipathic and as a consequence easily partition into the plasma membrane bilayer where they can elicit signaling effects on the molecular and supramolecular level. On the one hand, they can undergo bimolecular interactions with several proteins (enzymes) or, on the other hand, perturb a larger membrane area thus activating a series of proteins in a more unspecific manner. Sustained protein activation can be evoked by the phospholipid aldehyde POVPC. This compound alkylates proteins by Schiff base formation thereby improving their

association and interaction with membrane bilayers. Typical functional consequences have already been demonstrated by Kinnunen and colleagues. They found that Poxno-PC, a longer chain homologue of POVPC, improved phospholipase A_2 activity in artificial membranes and abolished the lag time that is usually observed with interfacially active enzymes (30). Other aldehydes have also been shown to activate membrane proteins in a covalent manner. For instance, modification of the epidermal growth factor receptor by hydroxynonenal mimics binding of its natural ligand thereby triggering specific signaling cascades (31,32). Finally, plasma membrane- bound oxPL may be released inside the cells where they can influence a number of other proteins/ enzymes directly.

Truncated phospholipids contain only one long hydrophobic fatty acid. As a consequence, they are highly exchangeable between lipid-water interfaces. Therefore, it is likely that the biological activities of PGPC and POVPC are due to multiple lipid-protein or lipid-lipid interactions rather than specific binding to a couple of receptors. In this study, we used fluorescently labeled derivatives of PGPC and POVPC to measure lipid uptake into cultured RAW 264.7 macrophages and identify their primary protein targets. The fluorescent lipids contained a BY- fluorophore bound to the polar head groups. They are reliable analogs of their natural counterparts. It has already been shown by the group of Berliner that the biological activities of truncated phospholipids are mainly determined by the structure of the polar *sn*-2 acyl chain and to a much lesser extent by the structure of the polar heads (33). We found that proper labeling of oxPL did not significantly alter their signaling effects. Head group-labeled analogs and unlabeled lipids elicited the same activation of aSMase generating the apoptotic lipid messenger ceramide (8,11). A comparative study on the inflammatory response of vascular cells towards oxPL and their biotin-labeled analogs also provided evidence that head-group labeling is not critical (34).

All these observations are in agreement with the assumption that the truncated oxPL mainly “communicate” at the membrane surface via their polar *sn*-2 acyl chains (see above).

Since we used fluorescent PGPC and POVPC analogs, we were able to study the time-dependent lipid uptake and localization in live cells reducing the probability of artefacts. In a previous study on the import of biotin-tagged oxPL into HAEC, cell fixation was required for lipid localization by secondary fluorescence staining of biotin (34). This stabilization is based on cross-linking by aldehydes which affects and perturbs (subcellular) membrane assemblies.

In agreement with previous studies, the fluorescent PGPC analog was quickly internalized by the cells (24). In contrast, POVPC was retained in the plasma membrane since it contains an aldehyde group which can form covalent Schiff bases with the amino groups of proteins and phospholipids. It is striking, especially in the case of POVPC, that delivery of the labeled phospholipids analogs to the cells did not depend on the lipid donor (aqueous lipid dispersions and lipid complexes with albumin and LDL).

Lipid complexes with albumin and LDL are likely to be physiologically relevant donors of oxPL *in vivo*. LDL is a site of lipid oxidation. Albumin may extract oxPL from the particle, since it shows binding affinities for phospholipids containing only one long hydrophobic fatty acid, e.g. lysolecithin (23). We were able to show that both carriers form stable complexes with fluorescent oxPL, too (Figure 2). Whereas PGPC only physically binds to proteins and lipoproteins, POVPC is covalently linked to these carriers. However, regardless of covalent binding, the POPVC analog is released from these donor systems to cells and vice versa. In addition, it is freely exchangeable between the individual donors. This exchangeability is due to the

instability of the covalent lipid adducts. The pK-values for Schiff bases around 7 (26) makes the imines prone to protonation and nucleophilic substitution by other amines. As a consequence, short-chain oxPL, including phospholipids aldehydes, are not only active at the site of their formation but can be spread as “signal transducers” to the near cellular environment by diffusion within the tissues as well as to tissues far distant from the site of oxidative stress via the circulation. The relevance of such processes has already been underscored by the identification of small particles in the circulation that are enriched in oxidized phospholipids (35,36).

We screened for the primary protein targets of aldehydo-phospholipids in cultured macrophages using a fluorescent POVPC analogue. This phospholipid forms covalent Schiff bases that can be stabilized by chemical reduction for further protein separation, detection and analysis. In contrast to our “expectations”, protein labeling by this compound was selective (Figure 6). A fluorescence image of the phospholipid- tagged proteins was much less complex than a total protein stain of the same cell lysate. A similar observation was made with a biotin-tagged oxidized phospholipid mixture in HAECs (34). We suppose that this selectivity is not due to specific molecular recognition but rather due to differences in the pK values of the individual amino groups of the target proteins. This value is influenced by surface exposure and interaction with membrane lipids and proteins in the immediate vicinity. A detailed analysis of the labeled target candidates led to the identification of proteins involved in cell death and survival, stress response, transport and lipid metabolism. There is some overlap between the protein targets detected by the biotin-tagged probes (34) and the fluorescent POVPC analog. However, many other proteins identified in our studies have not been reported in literature so far.

Protein modification by POVPC may lead to activation of apoptotic signaling components, as well as suppression of functions that help the cell survive. Here, we would like to put the emphasis on the potential roles of some target candidates that seem particularly relevant to POVPC-induced apoptosis. Cathepsin D, caspase 1 and caspase 3 are components of programmed cell death. Cathepsin D is a lysosomal protease which is also associated with endosomal membranes (37). Reactive oxygen species, oxidized proteins and lipids have already been shown to activate this enzyme and increase the level of p53 which is a transcription factor for Cathepsin D. Activation of this protease leads to cytochrome c release from mitochondria, caspase 3 activation and cell death (38). Heat shock protein Hsp70B is expressed and released by macrophages in response to oxidized LDL which is a carrier of oxPL. This protein plays a key role in the activation of macrophages and helps the cells survive under oxidative stress (39). Calcium channels have also been identified as targets of oxPL and play a role in atherosclerosis (40). Voltage dependent anion channel 1 (VDAC 1) is involved in mitochondria-mediated apoptosis by regulating cytochrome c release (41). mmLDL rich in oxPL induces formation of reactive oxygen species leading to proinflammatory cytokine expression. This process also depends on a target identified in this study, namely spleen tyrosine kinase. Bae et al. found that this enzyme is activated by mmLDL downstream of TLR 4 leading to ROS generation in macrophages (42). TLR 4 signaling is inhibited by oxPL (43), due to disruption of lipid rafts in the plasma membrane. This phenomenon is in line with results from single molecule fluorescence microscopy showing that fluorescent oxPL (PGPC) partition into lipid raft-like membrane domains (caveolae) (24). In this context, it is interesting to note that Stomatin has also been identified as a POVPC target.

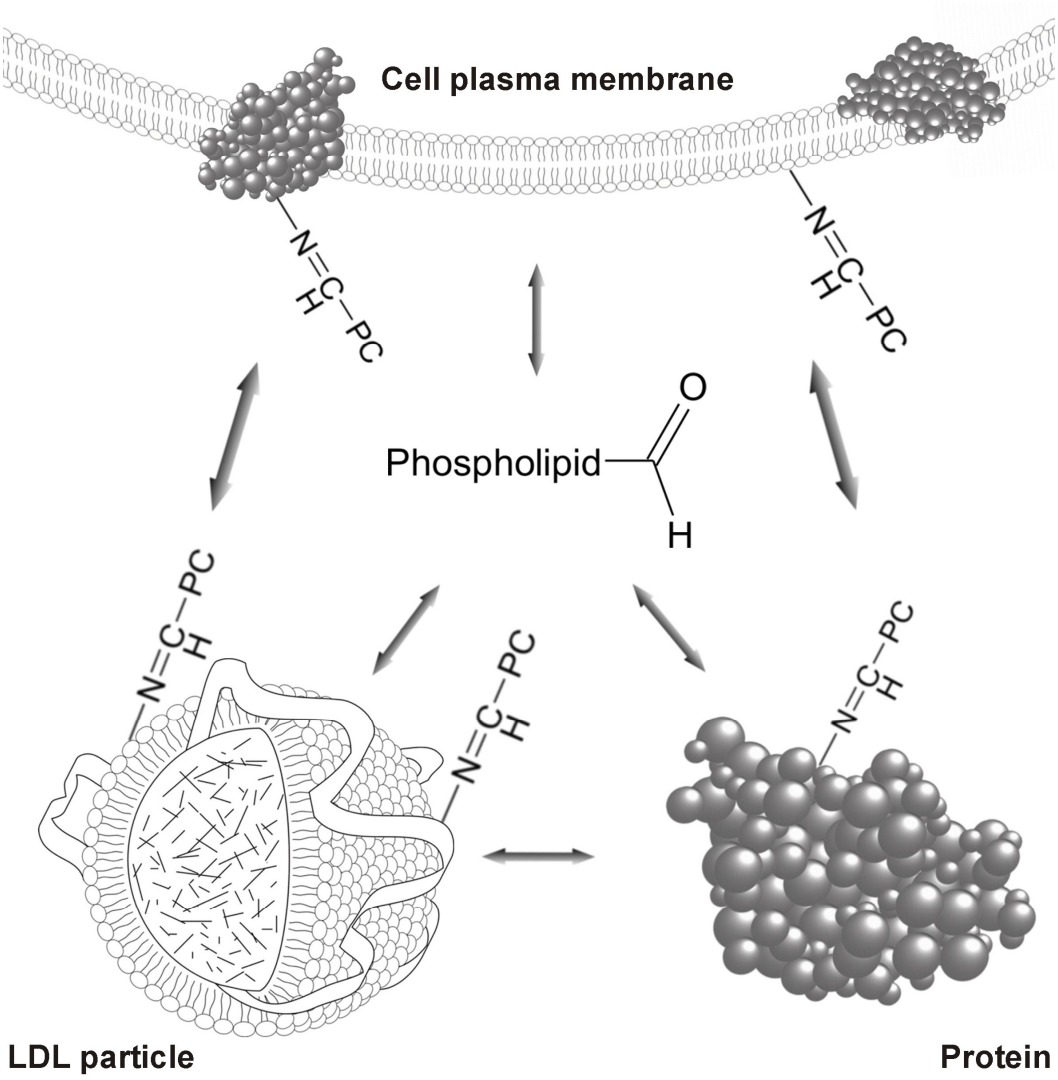

Figure 7: Exchange of BY- POVPE between lipid-protein surfaces

OxPL, including POVPC, may be bound to at least three physiologically relevant carriers. The respective supramolecular systems are lipid aggregates (aqueous lipid suspension), complexes with proteins (BSA) and lipoproteins (LDL). POVPC forms covalent Schiff bases with the amino groups of phospholipids and proteins. Despite the fact that the oxPL is firmly bound to these molecules (see Figure 2), it is released to lipids and proteins of the cell plasma membrane. In addition, POVPC is easily released from its albumin complex and to a lower extent from its LDL complex (see Figure 3 and 4), too, if other lipid acceptors are present. The exchangeability of the covalently bound aldehydo lipid can be explained by the pKs of aliphatic Schiff bases around pK 7. At this pK, a significant fraction of the imine is protonated and thus subject to nucleophilic substitution by other amines. LDL showed the highest affinity for POVPC binding (accommodation in the phospholipids monolayer and binding by apoB) and can thus be considered the main carrier for delivery of the oxPL to the cells.

This protein belongs to a larger family of polypeptides sharing an evolutionary conserved stomatin/ prohibitin/ flotilin/ HflK/ C domain (44). It is known from studies on epithelial cells (45), erythrocytes (46) and platelet alpha granules (47) that it is a major raft component. N-acyl-sphingosine hydrolase (ceramidase) and sphingosine phosphate lyase are also potential POVPC targets. They are involved in sphingolipid metabolism and influence the ceramide concentrations and cell susceptibility to apoptosis (48).

We have preliminary evidence that POVPC forms covalent adducts not only with proteins but also with aminophospholipids in cell membranes. Incubation of BY-POVPE with cultured cells led to the formation of two new fluorescent phospholipids with lower polarity. The structures of these compounds are currently subject to identification.

In summary, we have shown that fluorescent analogs of PGPC and POVPC are easily taken up into macrophages irrespective of the lipid donor. Whereas POVPC is initially scavenged by covalent reaction with the components of the plasma membrane, PGPC is quickly internalized. Despite the covalent binding to its lipid and protein targets, POVPC is freely exchangeable between membranes and (lipo-) protein surfaces. As a consequence, this lipid represents a toxic compound which is active not only at the site of its formation but also in cells far distant from areas of oxidative stress (Figure 7). The identification of the potential POVPC protein targets supports the assumption that POVPC interacts with multiple sites and not only with the traditional specific receptors.

Current studies are on the way to identify the functional proteins that represent the primary signaling platforms of cell death induced in macrophages by oxPL.

6. ABBREVIATIONS

aSMase: acid sphingomyelinase

BSA: bovine serum albumin

BY: BODIPY™

DMEM: Dulbeccos modified eagle medium

FRET: Förster resonance energy transfer

HAEC: human aortic endothelial cells

IL: interleukin

LDL: low-density lipoprotein

MAPK: mitogen-activated protein kinase

mmLDL: minimally modified low-density lipoprotein

oxLDL: oxidized low- density lipoprotein

oxPL: oxidized phospholipids

PAF: platelet activating factor

PAPC: 1-palmitoyl-2-arachidonoyl-sn-glycero-3-phosphocholine

Paze-PC: 1-palmitoyl-2-azelaoyl-ns-glycero-3-phosphocholine

PC: phosphatidylcholine

PE: phosphatidylethanolamine

PGPC: 1-palmitoyl-2-glutaroyl -sn-glycero-3-phosphocholine

POPE: 1-palmitoyl-2-oleoyl-sn-glycero-3-phosphoethanolamine

POVPC: 1-palmitoyl-2-(5-oxovaleroyl)-sn-glycero-3-phosphocholine

Poxno-PC: 1-palmitoyl-2-(9'oxo-nonanoyl)-sn-glycero-3-phosphocholine

PS: phosphatidylserine

ROS: reactive oxygen species

TCA: trichloroacetic acid

TLC: thin layer chromatography

TLR: toll-like receptor

VDAC: voltage dependent anion channel

7. ACKNOWLEDGEMENT

This work was financially supported by the Austrian Science Fund FWF (project F30-B05 - special research program SFB *Lipotox*) and ESF EuroMEMBRANE CRP OXPL (project I308-B12). The authors wish to thank Dr. Gholam Ali Khoschsorur (University Hospital Graz, Austria) for providing us with pooled blood plasma samples and Dr. Dagmar Kratky (Medical University, Graz, Austria) for providing the RAW 264.7 cells.

8. REFERENCE LIST

1. Steinberg, D. (2009) *J.Lipid Res.* **50 Suppl,** S376-S381
2. Gillotte, K. L., Horkko, S., Witztum, J. L., and Steinberg, D. (2000) *J.Lipid Res.* **41,** 824-833
3. Deigner, H. P. and Hermetter, A. (2008) *Curr.Opin.Lipidol.* **19,** 289-294
4. Fruhwirth, G. O. and Hermetter, A. (2008) *Subcell.Biochem.* **49,** 351-367
5. Fruhwirth, G. O., Loidl, A., and Hermetter, A. (2007) *Biochim.Biophys.Acta* **1772,** 718-736
6. Mertens, A. and Holvoet, P. (2001) *FASEB J.* **15,** 2073-2084
7. Fruhwirth, G. O., Moumtzi, A., Loidl, A., Ingolic, E., and Hermetter, A. (2006) *Biochim.Biophys.Acta* **1761,** 1060-1069
8. Loidl, A., Sevcsik, E., Riesenhuber, G., Deigner, H. P., and Hermetter, A. (2003) *J.Biol.Chem.* **278,** 32921-32928
9. Khandelia, H. and Mouritsen, O. G. (2009) *Biophys.J.* **96,** 2734-2743
10. Smiley, P. L., Stremler, K. E., Prescott, S. M., Zimmerman, G. A., and McIntyre, T. M. (1991) *J.Biol.Chem.* **266,** 11104-11110
11. Moumtzi, A., Trenker, M., Flicker, K., Zenzmaier, E., Saf, R., and Hermetter, A. (2007) *J.Lipid Res.* **48,** 565-582
12. Chung, B. H., Wilkinson, T., Geer, J. C., and Segrest, J. P. (1980) *J.Lipid Res.* **21,** 284-291
13. Bradford, M. M. (1976) *Anal.Biochem.* **72,** 248-254

14. Watson, A. D., Leitinger, N., Navab, M., Faull, K. F., Horkko, S., Witztum, J. L., Palinski, W., Schwenke, D., Salomon, R. G., Sha, W., Subbanagounder, G., Fogelman, A. M., and Berliner, J. A. (1997) *J.Biol.Chem.* **272,** 13597-13607

15. Batzri, S. and Korn, E. D. (1973) *Biochim.Biophys.Acta* **298,** 1015-1019

16. Wessel, D. and Flugge, U. I. (1984) *Anal.Biochem.* **138,** 141-143

17. Fling, S. P. and Gregerson, D. S. (1986) *Anal.Biochem.* **155,** 83-88

18. Gorg, A., Obermaier, C., Boguth, G., Harder, A., Scheibe, B., Wildgruber, R., and Weiss, W. (2000) *Electrophoresis* **21,** 1037-1053

19. Shevchenko, A., Wilm, M., Vorm, O., and Mann, M. (1996) *Anal.Chem.* **68,** 850-858

20. Birner-Grunberger, R., Scholze, H., Faber, K., and Hermetter, A. (2004) *Biotechnol.Bioeng.* **85,** 147-154

21. Carr, S., Aebersold, R., Baldwin, M., Burlingame, A., Clauser, K., and Nesvizhskii, A. (2004) *Mol.Cell Proteomics.* **3,** 531-533

22. Ravandi, A., Kuksis, A., Shaikh, N., and Jackowski, G. (1997) *Lipids* **32,** 989-1001

23. Brown, S. D., Baker, B. L., and Bell, J. D. (1993) *Biochim.Biophys.Acta* **1168,** 13-22

24. Rhode, S., Grurl, R., Brameshuber, M., Hermetter, A., and Schutz, G. J. (2009) *J.Biol.Chem.* **284,** 2258-2265

25. Chen, C. H. (2004) *Curr.Opin.Lipidol.* **15,** 337-341

26. Sheves, M., Albeck, A., Friedman, N., and Ottolenghi, M. (1986) *Proc.Natl.Acad.Sci.U.S.A* **83,** 3262-3266

27. Pegorier, S., Stengel, D., Durand, H., Croset, M., and Ninio, E. (2006) *Atherosclerosis* **188,** 433-443

28. Seimon, T. A., Nadolski, M. J., Liao, X., Magallon, J., Nguyen, M., Feric, N. T., Koschinsky, M. L., Harkewicz, R., Witztum, J. L., Tsimikas, S., Golenbock, D., Moore, K. J., and Tabas, I. (2010) *Cell Metab* **12,** 467-482

29. Greenberg, M. E., Li, X. M., Gugiu, B. G., Gu, X., Qin, J., Salomon, R. G., and Hazen, S. L. (2008) *J.Biol.Chem.* **283,** 2385-2396

30. Code, C., Mahalka, A. K., Bry, K., and Kinnunen, P. K. (2010) *Biochim.Biophys.Acta* **1798,** 1593-1600

31. Esterbauer, H., Schaur, R. J., and Zollner, H. (1991) *Free Radic.Biol.Med.* **11,** 81-128

32. Uchida, K., Szweda, L. I., Chae, H. Z., and Stadtman, E. R. (1993) *Proc.Natl.Acad.Sci.U.S.A* **90,** 8742-8746

33. Subbanagounder, G., Leitinger, N., Schwenke, D. C., Wong, J. W., Lee, H., Rizza, C., Watson, A. D., Faull, K. F., Fogelman, A. M., and Berliner, J. A. (2000) *Arterioscler.Thromb.Vasc.Biol.* **20,** 2248-2254

34. Gugiu, B. G., Mouillesseaux, K., Duong, V., Herzog, T., Hekimian, A., Koroniak, L., Vondriska, T. M., and Watson, A. D. (2008) *J.Lipid Res.* **49,** 510-520

35. Huber, J., Vales, A., Mitulovic, G., Blumer, M., Schmid, R., Witztum, J. L., Binder, B. R., and Leitinger, N. (2002) *Arterioscler.Thromb.Vasc.Biol.* **22,** 101-107

36. Huber, L. C., Jungel, A., Distler, J. H., Moritz, F., Gay, R. E., Michel, B. A., Pisetsky, D. S., Gay, S., and Distler, O. (2007) *Apoptosis.* **12,** 363-374

37. Diment, S., Leech, M. S., and Stahl, P. D. (1988) *J.Biol.Chem.* **263,** 6901-6907

38. Kagedal, K., Johansson, U., and Ollinger, K. (2001) *FASEB J.* **15,** 1592-1594

39. Smith, K. J., Twal, W. O., Soodavar, F., Virella, G., Lopes-Virella, M. F., and Hammad, S. M. (2010) *J.Biol.Chem.* **285,** 15985-15993

40. Al-Shawaf, E., Naylor, J., Taylor, H., Riches, K., Milligan, C. J., O'Regan, D., Porter, K. E., Li, J., and Beech, D. J. (2010) *Arterioscler.Thromb.Vasc.Biol.*

41. bu-Hamad, S., Arbel, N., Calo, D., Arzoine, L., Israelson, A., Keinan, N., Ben-Romano, R., Friedman, O., and Shoshan-Barmatz, V. (2009) *J.Cell Sci.* **122,** 1906-1916

42. Bae, Y. S., Lee, J. H., Choi, S. H., Kim, S., Almazan, F., Witztum, J. L., and Miller, Y. I. (2009) *Circ.Res.* **104,** 210-8, 21p

43. Erridge, C., Kennedy, S., Spickett, C. M., and Webb, D. J. (2008) *J.Biol.Chem.* **283,** 24748-24759

44. Liu, J., Deyoung, S. M., Zhang, M., Dold, L. H., and Saltiel, A. R. (2005) *J.Biol.Chem.* **280,** 16125-16134

45. Snyers, L., Umlauf, E., and Prohaska, R. (1999) *Eur.J.Cell Biol.* **78,** 802-812

46. Salzer, U. and Prohaska, R. (2001) *Blood* **97,** 1141-1143

47. Mairhofer, M., Steiner, M., Mosgoeller, W., Prohaska, R., and Salzer, U. (2002) *Blood* **100,** 897-904

48. Reiss, U., Oskouian, B., Zhou, J., Gupta, V., Sooriyakumaran, P., Kelly, S., Wang, E., Merrill, A. H., Jr., and Saba, J. D. (2004) *J.Biol.Chem.* **279,** 1281-1290